The Dark Energy Spectrometer (DESpec): A Multi-Fiber Spectroscopic Upgrade of the Dark Energy Camera and Survey for the Blanco Telescope

March 29, 2012

F. Abdalla, J. Annis, D. Bacon, G. Bernstein, S. Bridle, F. Castander, M. Colless, D. DePoy, H. T. Diehl, R. Ellis, B. Flaugher, J. Frieman, E. Gaztanaga, B. Gerke, C. Hogan, B. Jain, S. Jouvel, S. Kent, D. Kirk, R. Kron, S. Kuhlmann, O. Lahav, J. Lawrence, H. Lin, J. Marriner, J. Marshall, J. Mohr, R. Nichol, M. Sako, W. Saunders, M. Seiffert, D. Thomas, R. Wechsler, A. West, H. Wu

Draft: Do not circulate

Abstract

We describe a new initiative to build and operate the Dark Energy Spectrometer (DESpec), a wide-field, deep spectroscopic survey instrument for the Blanco 4-meter telescope at Cerro Tololo Inter-American Observatory (CTIO) in Chile. A new robotic system with about 4000 optical fibers will interchangeably replace the CCD imager of the existing Dark Energy Camera (DECam), accessing a field of view of 3.8 sq. deg. In a survey of ~300 nights, the DESpec collaboration proposes to obtain spectroscopic redshifts for ~7 million galaxies over 5000 sq. deg. selected from precision imaging by the Dark Energy Survey (DES). Under reasonable assumptions, the 5000 sq. deg. DESpec survey, in combination with DES itself, will improve the Dark Energy Task Force (DETF) Figure of Merit by a factor of several over DES, reaching the level for a Stage IV DETF project. Since it adds a spectroscopic third dimension to the *same sky* as DES, the world's largest and deepest photometric survey, DESpec will enable a powerful array of new statistical techniques to discriminate among alternative explanations of cosmic acceleration, such as Dark Energy and Modified Gravity. In the LSST era, a wider-area DESpec spectroscopic survey will greatly enhance the science reach of LSST, providing spectroscopic follow-up for tens of millions of LSST targets over its 15,000-20,000 sq. deg. survey area. DESpec will take advantage of the substantial hardware infrastructure recently built for DECam to achieve excellent science at low cost and low technical and schedule risk. DESpec will be mounted in the DECam prime focus cage and will be routinely interchangeable with the DECam CCD imager to allow flexible use of the telescope. It will share the four largest DECam optical corrector elements and feature a focal plane with robotically positioned optical fibers feeding up to 10 high-throughput spectrometers outfitted with existing, spare, red-sensitive, science-grade DECam CCDs. A simple, single-arm design option offers a wavelength range of 600-1000 nm and a spectral resolution of R=3334 at λ=1000 nm. A two-arm spectrograph design could achieve increased wavelength range and greater spectral resolution. An Atmospheric Dispersion Compensator similar to existing designs is easily accommodated in the DECam filter slot. DESpec in the south would complement and have comparable survey power to the proposed BigBOSS in the north; together they would form a powerful, all-sky spectroscopic system.

1. Introduction & Executive Summary

In 1998, two teams of astronomers studying distant Type Ia supernovae presented evidence that the expansion of the Universe is speeding up rather than slowing down due to gravity (Riess, et al. 1998, Perlmutter, et al. 1999), arguably the most important discovery in cosmology of the last 30 years. Observations since then of supernovae, large-scale structure, the cosmic microwave background, and galaxy clusters have confirmed this remarkable finding (e.g., Frieman, Turner, & Huterer 2008, Sullivan, et al. 2011). The physical origin of cosmic acceleration remains a mystery; unraveling it will have profound implications for fundamental physics and will be an important goal for coming years, as highlighted most recently by the National Academy of Science's Astronomy and Astrophysics Decadal Survey Report: New Worlds, New Horizons (2010). Is acceleration caused by Dark Energy (DE), a new form of stress-energy with negative effective pressure, $w=p/\rho<-1/3$, that makes up 70% of the Universe, or does it indicate that Einstein's Theory of General Relativity (GR) must be replaced by a new theory of gravity on cosmic scales? If the answer is dark energy, is it the energy of the vacuum---or equivalently the cosmological constant (for which $w=-1$)---or something else, perhaps an ultralight scalar field sometimes dubbed quintessence?

Our best tools for addressing these questions are measurement of the history of the cosmic expansion rate and of the growth of large-scale structure. If General Relativity plus dark energy is the correct paradigm, then there is a definite correlation between the expansion rate and the growth of structure. While the current data are consistent with vacuum energy as the cause of cosmic acceleration, we need more precise measurements to draw definitive conclusions about the nature of dark energy and the consistency of the GR+DE paradigm.

A major advance in this program will come soon from the Dark Energy Survey (DES), a deep, wide, multi-band imaging survey, spanning 525 nights over five years beginning in late 2012, that will use the new 570-Megapixel Dark Energy Camera on the Blanco 4-m telescope at CTIO (DES Collaboration, 2005). DES, in partnership with ESO's near-infrared VISTA Hemisphere Survey (VHS), will provide imaging of ~200 million galaxies in 5+3 optical-NIR filters (grizY for DES, JHK for VHS) over 5000 sq. deg. DES will also discover and measure ~4000 SN Ia light curves in a time-domain survey of 30 sq. deg. With this survey, DES will probe dark energy using four techniques: the clustering of galaxies on large scales, including baryon acoustic oscillations (BAO); the abundance of massive galaxy clusters; weak gravitational lensing distortions of the images of distant galaxies; and Type Ia supernova distances. DES is an international collaboration, with over 120 senior scientists from 26 institutions in the US, the UK, Spain, Brazil, and Germany. Funding for the DES within the US is provided by the Department of Energy (DOE), the National Science Foundation (NSF), and the participating institutions. In the language of the Dark Energy Task Force report (DETF, Albrecht, et al. 2006), DES is a `Stage III' experiment that will make a substantial step forward in constraining the properties of dark energy.

Draft. Do not circulate

As a multi-band imaging survey, DES (and later LSST) will provide precise measurements of galaxy fluxes, colors, and shapes but only approximate photometric estimates of their redshifts (photo-z's). High-precision redshifts, which enable a true 3d map of the cosmos, require spectroscopy. The DESpec collaboration seeks to substantially enhance the science reach of DES imaging, and better probe the origin of cosmic acceleration, by obtaining spectroscopic redshifts for a large sample of DES target galaxies, yielding a dense sampling of 3d structure over the wide, deep volume probed by DES.

The need for such data has led us to explore DESpec, a concept for a ~4000-fiber spectrograph for the Blanco telescope, which would enable a ~7 million galaxy survey in ~300 nights. We consider DESpec an `upgrade' of the Dark Energy Camera and of the DES project, following the model of upgrades that enhance the capabilities of high-energy particle physics experiments. Together with DES, DESpec would have the science reach of a next-generation, DETF Stage IV project. Once LSST begins survey operations from neighboring Cerro Pachon, the DESpec survey could be expanded to ~15,000 sq. deg., yielding redshifts for ~20 million galaxies in ~900 nights and substantially enhancing the science reach of LSST. This sample is comparable to and would complement the proposed BigBOSS survey in the north (Schlegel, et al. 2011; see Appendix).

The unique strength of the DESpec survey transcends the statistics captured in the DETF figure of merit: it will provide a 3d redshift map of the Universe over the same deep, wide volume precisely mapped by DES and later LSST. The statistical versatility and power of a comprehensive, deep 3d survey coupled with a precision, multi-band photometric survey was demonstrated by the Sloan Digital Sky Survey (SDSS), which was instrumental in establishing the current cosmological paradigm. To probe the physical origin of cosmic acceleration will require a combination of many statistical techniques, only some of which are now known and well tested. DESpec will extend that capability to a volume roughly 5 times deeper and 50 times larger than SDSS, extending back to an era before Dark Energy ruled the cosmos. DESpec enables a wide range of DE probes that powerfully synergize in ways that no other foreseen spectroscopic surveys can achieve.

The spectroscopic redshift information that DESpec adds to the DES(+VHS) galaxy catalog results in a substantial increase in the precision of the dark energy equation of state parameter, w, and its time evolution, dw/da, from all four of the techniques above. Spectroscopic redshift precision also enables qualitatively new dark energy probes beyond DES, for example, radial baryon acoustic oscillations and redshift-space distortions (RSD). It can also provide dynamical mass estimates for thousands of DES galaxy clusters, strengthening the cluster probe of DE. Redshift data also increase the power of weak lensing as a probe. In the southern hemisphere, this includes cross-correlation with lensing of the microwave background radiation, now detected in high resolution imaging by the South Pole Telescope and the Atacama Cosmology Telescope.

Draft. Do not circulate

Among the many new capabilities enabled by DESpec, one exciting recent realization is that the combination of redshift distortions from DESpec and weak lensing from DES (and later LSST) can powerfully discriminate models of Modified Gravity from Dark Energy as the cause of cosmic acceleration (Zhang, et al. 2007, Guzik, et al. 2009, Song & Dore 2009, Reyes, et al. 2010, Song, et al. 2011), *with reduced uncertainty due to galaxy bias and cosmic variance if the photometric and spectroscopic surveys cover the same sky area* as DES and DESpec would do (Pen 2004, McDonald & Seljak 2009, Bernstein & Cai 2011, Cai & Bernstein 2011, Gaztanaga, et al. 2011). Further, the DESpec survey can set a strict upper limit on or even detect the mass of neutrinos, with expected sensitivity of ~0.05 eV in combination with DES and Planck, highly competitive with laboratory experiments. This very large spectroscopic survey will also probe the presently puzzling excess power in the galaxy clustering power spectrum on the Gigaparsec scale (Thomas, Abdalla, & Lahav 2011) and enable new studies of galaxy evolution and of quasars. Additional payoffs include reducing DES weak lensing intrinsic alignment systematics by cross-correlating the lensing shear signal with a spectroscopic galaxy sample, detailed study of the dark matter environments of galaxies and clusters via stacked weak lensing mass estimates, and measurement of cluster dynamical masses via velocity dispersions. These arguments are strengthened when extended to wider-area follow-up of LSST imaging.

A unique advantage of this project is the uniform, deep target list of objects with precision multi-band photometry and lensing shape measurements that will come from DES and the ability to access the entire sky area that will be surveyed by both DES (5000 sq. deg.) and LSST (20,000 sq. deg.). Located in the southern hemisphere at one of the world's premier astronomical sites (CTIO has a median site seeing of 0.65" FWHM and 80% useable nights), DESpec would yield a wealth of spectroscopic information complementary to the larger-aperture, narrower-field VLT, Gemini, Magellan, and other telescopes concentrated in the southern hemisphere. In the long term, it would enable massively parallel follow-up to LSST (and possibly Euclid and/or WFIRST) imaging surveys.

In addition to its dark energy goals, as a community instrument DESpec would enable a wide array of spectroscopic surveys that would afford opportunities for discoveries in stellar structure and evolution, nearby galaxies, galaxy evolution, the structure of galaxy clusters, and beyond. Given the large number of fibers, building on the experience of the Sloan Digital Sky Survey, one could optimize efficiency by conducting many survey programs in parallel. The ability to interchange the instrument with DECam enables a flexible observing program including wide field imaging in the pre-LSST era. This program efficiently exploits the unique wide field and structural capabilities of the Blanco telescope. The DESpec/DECam system creates an opportunity for optimal use of resources by both DOE and NSF user communities: a large science impact per dollar and a beneficial partnership combining the technical resources of both agencies. Moreover, in the LSST era, the wide-field spectroscopic capability of DESpec would complement two other capabilities---one following up very faint LSST sources over small sky

Draft: Do not circulate

areas (e.g., with ~8 to 30-meter telescopes and with JWST) and the other following up optical LSST transients on very rapid timescales---to form an optimized southern spectroscopic system.

DESpec achieves relatively low cost, schedule, and technical risk by capitalizing on and leveraging the recent investment in DECam and recent structural improvements in the Blanco telescope and its environment made by NOAO (new primary mirror radial supports, improved telescope control system, and environmental control). It uses the DECam mechanical structure (prime focus cage, barrel, shutter, hexapod alignment system), four of the same corrector lenses, and an ample supply (~60) of existing spare, packaged and tested, red-sensitive, science-grade 2kx4k CCDs produced for the DECam project. Two or three new optical corrector elements will be needed, including two lenses and possibly an Atmospheric Dispersion Compensator. The resulting optical beam is nearly telecentric. The preliminary design entails ~4000 robotically positioned optical fibers of diameter 1.4" (80 microns) over the existing DECam 3.8 sq. deg. field of view, feeding 10 single-arm spectrographs.

One low per-instrument cost design builds upon that used for the Hobby-Eberly Telescope Dark Energy Experiment (HETDEX). The CCD readout electronics will be copied from the low-read-noise DECam design, again saving cost and reducing risk. The wavelength range of the spectrographs will be approximately 600 to 1000 nm, with a spectral resolution of $R=\lambda/\Delta\lambda=3334$ at 1000 nm. Over this range, the optical corrector produces an appropriately small spot size of 0.4-0.63" FWHM. All of the preceding design numbers (fiber size, wavelength range, spectral resolution, and resulting spectrograph design) will be optimized in the R&D phase. Since NOAO expects to operate DECam for at least five years beyond the end of DES (i.e., to 2022), DESpec will be designed to be interchangeable with DECam on a timescale of a few days or less.

A three-year R&D program for DESpec will focus on: (1) optimizing the optical and spectrograph design, balancing science requirements against cost and schedule and demonstrating feasibility; (2) establishing requirements for and demonstrating technological feasibility of the fiber-positioning system---the groups developing the Echidna and COBRA fiber-positioning systems have built prototype systems that appear to meet our requirements; (3) building upon DECam expertise to complete design of the CCD readout electronics and mechanical design. The R&D will produce a final design and construction cost and schedule estimate. The collaboration will seek project funding from the US agencies DOE and NSF (with major hardware funding to be proposed to the DOE), international funding agencies, and the participating institutions, following the successful model of the DES project. It is expected that a number of DES and non-DES institutions will participate. There is substantial interest in the project from foreign institutions, and the UK STFC recently awarded a grant for DESpec R&D. We will propose that the instrument be operated by the National Optical Astronomy Observatory (NOAO), which operates CTIO, under a time allocation agreement with the collaboration to be negotiated (as was done for DES, which was allocated 525 nights in exchange for DECam). However, we note that NOAO has not issued nor indicated that they will issue an announcement of opportunity for a new instrument for the Blanco Telescope.

Draft: Do not circulate

Section 2 of this White Paper outlines the science case for DESpec, focusing on probes of dark energy and tests of General Relativity. Section 3 discusses the selection of galaxy spectroscopic targets and defines a strawman survey strategy that follows from the science requirements of Sec. 2. Section 4 discusses the DESpec instrument components, highlighting those areas that would be addressed in the R&D phase, and we conclude in Sec. 5. An appendix briefly compares DESpec with the proposed BigBOSS project.

2. DESpec Science Program

2.A. Probing the origin of cosmic acceleration and testing General Relativity

The Dark Energy Survey (DES) will enable measurements of the dark energy and dark matter densities and of the dark energy equation of state through four methods: galaxy clusters, weak gravitational lensing (WL), galaxy angular clustering (including angular Baryon Acoustic Oscillations, BAO), and supernovae (SNe). A spectroscopic redshift survey of a substantial fraction of DES target galaxies with an instrument such as DESpec would enhance each of these techniques, particularly the measurement of baryon acoustic oscillations (BAO) through galaxy clustering, and enable a new DE probe, redshift-space distortions (RSD). Moreover, the combination of RSD from DESpec with WL from DES and subsequently LSST would enable a powerful new test of the consistency of the General Relativity-plus-Dark Energy paradigm and therefore help distinguish Dark Energy from Modified Gravity as the physical cause of cosmic acceleration.

To frame the discussion, we outline the DES survey and a strawman concept for the DESpec survey---the latter is more fully discussed in Sec. 3---and introduce figures of merit for DE and parameters for testing departures from General Relativity.

The DES will comprise two multi-band imaging surveys, a wide-field survey and a narrow time-domain survey. The wide-field survey will nominally cover 5000 sq. deg. in the south Galactic cap, all at high galactic latitude suitable for extragalactic studies, reaching ~24^{th} magnitude in the grizY filters. The depth and filter coverage of the wide-field survey were chosen primarily to achieve accurate galaxy and cluster photo-z measurements to redshifts z>1. The wide-field survey will detect over 100,000 galaxy clusters and measure shapes, photo-z's, and positions for ~300 million galaxies. It will overlap completely with the ESO Vista Hemisphere Survey (VHS), which will obtain moderately deep imaging in J, H, and K filters. The combined 8-filter data will extend the range of precise galaxy photo-z's to z~2. The DES Supernova Survey involves frequent (every few days) imaging of a 30 sq. deg. area in the riz filters, which will yield well-measured light curves for ~4000 Type Ia supernovae to redshifts z~1.

The DETF defined a figure of merit (FoM) for dark energy surveys by parametrizing the redshift evolution of the dark energy equation of state parameter by $w(a)=w_0+w_a(1-a)$, where $a(t)=1/(1+z)$ is the cosmic scale factor, w_0 is the current value of w, and w_a is a measure of its

Draft. Do not circulate

evolution with redshift. The DETF FoM is proportional to the reciprocal of the area in the w_0-w_a plane that encloses the 95% CL region. Defining a pivot epoch, a_p, at which the uncertainty in $w(a)$ is minimized for a given experiment, the DETF FoM is $[\sigma(w_p)\sigma(w_a)]^{-1}$. More complex figures of merit have also been proposed (Albrecht & Bernstein 2007, Albrecht, et al. 2009). The DETF report provided an estimate for the Stage II FoM of about 60, where Stage II includes projections from surveys that were on-going at the time the report was written, combined with the forecast statistical precision of Planck CMB measurements on cosmological parameters. Using similar techniques, the DES collaboration estimated a combined FoM from all four techniques of about 260 for the final survey, characteristic of a DETF Stage III project. There is considerable uncertainty in this forecast, since there are large uncertainties in the ultimate levels of systematic errors for each of the techniques. According to the DETF, next-generation, Stage IV projects would be anticipated to increase the DETF FoM by another factor of ~3-5 compared to DES+Planck. Our initial projections indicate that the DES+DESpec combination would reach that level of precision.

In testing Modified Gravity (MG) vs. Dark Energy, it is also useful to have parameters and FoMs describing departures from General Relativity, and several have been proposed. In GR+DE, the linear growth rate of linear density perturbations $\delta(a)$ that form large-scale structure is uniquely determined by the expansion rate $H(a)$ and the matter density parameter Ω_m. In particular, the logarithmic growth rate is given by $f(a)=d\ln\delta/d\ln a=\Omega_m(a)^\gamma$, where the growth exponent γ=0.55 in GR. In Modified Gravity theories, the relation between expansion history and perturbation growth can be changed; e.g., in the DGP braneworld model (Dvali, et al. 2000), γ=0.68. One FoM for modified gravity models is therefore $[\sigma(\gamma)]^{-2}$.

In a more general approach to Modified Gravity, in the Newtonian gauge describing scalar cosmological density perturbations, the perturbed spacetime metric can be written as

$$ds^2 = -[1+2\Psi(\vec{x},t)]dt^2 + a^2(t)[1-2\Phi(\vec{x},t)][d\chi^2 + r^2(\chi)d\Omega^2],$$

where Ψ and Φ denote the metric potentials. In GR in the absence of anisotropic stress, both of these `potentials' satisfy the Poisson equation, and thus $\Psi=\Phi$. In a class of MG theories, we can write the Fourier-space Poisson equation in comoving coordinates as

$$k^2\Psi = 4\pi G a^2 \mu(a,k)\bar{\rho}\delta(k,a)$$

where $\bar{\rho}$ is the mean matter density of the Universe, and $\mu=1$ in GR but may differ from unity and be time- and scale-dependent in a MG theory; μ can be thought of as a measure of the departure of the gravitational `constant' from its Newtonian value, $\mu=G/G_N$. In this description, the other MG parameter can be taken to be $\eta(a,k)=\Phi/\Psi$ ($=1$ in GR). The deflection of light and therefore measures of gravitational lensing are determined by the sum $\Phi+\Psi$ (for a given mass distribution), i.e., the light deflection angle is given by $\alpha = \nabla_\perp(\Phi+\Psi)$, where the derivative is

Draft. Do not circulate

taken transverse to the light path. On the other hand, the linear growth of density perturbations *f(a)* is sensitive only to the Newtonian potential Ψ or alternatively to μ, since the growth of non-relativistic matter perturbations satisfies the Fourier-space equation of motion

$$\ddot{\delta}(a,k) + 2H(a)\dot{\delta}(a,k) - \frac{k^2}{a^2}\Psi = 0$$

Comparing the effect of gravity on photons (via lensing) to the effect of gravity on matter (via, e.g., galaxy velocity surveys) therefore tests the equivalence of Φ and Ψ predicted by GR. Zhang, et al. (2007, 2008) proposed a specific comparison that determines $\mu(1+\eta)$. An initial estimate from the SDSS finds agreement with GR with ~15% error (Reyes, et al. 2010, see also Zhao, et al. 2010), but DES+DESpec would enable much more precise tests.

In addition to dark energy and modified gravity, DES+DESpec would probe other areas of fundamental physics, including neutrinos and primordial non-Gaussianity from inflation. Current constraints on the sum of neutrino masses from large-scale structure depend somewhat on details and assumptions of the analyses, but a relatively conservative recent analysis finds an upper bound of 0.28 eV at 95% CL (Thomas, Abdalla, and Lahav 2010), and DES+Planck is expected to reach 0.1 eV (Lahav, et al. 2010). We estimate that DES+DESpec clustering measurements plus Planck would improve this bound to ~0.05 eV, reaching the regime where neutrino oscillation experiments indicate a detection is likely. Measurement of large-scale clustering in DES+DESpec, particularly constraints on the scale-dependence of galaxy bias, will constrain departures from primordial Gaussianity and thereby test models of primordial inflation.

For our baseline DESpec survey, we assume ~7 million successful redshifts are acquired over the 5000 sq. deg. DES footprint. By using flux, colors, and surface brightness to target a mixture of Luminous Red Galaxies (LRGs) at $z<1$ and Emission Line Galaxies (ELGs) at redshifts $0.6<z<1.7$, we assume for purposes of illustration that the redshift distribution can be sculpted to be approximately constant over the redshift range $0.2<z<1.5$. Sec. 3 describes how such a selection could be carried out. An extended DESpec survey would extend this targeting to ~20 million galaxies over 15,000 sq. deg. of extragalactic sky, by selecting targets from LSST, which plans to survey 20,000 sq. deg. We note that, once it is operational, LSST will immediately reach the depth needed for selecting DESpec targets over its full survey area. We emphasize that this survey plan is just a strawman; the final target selection for DESpec (redshift distribution, flux limits, color selection, mix of LRG and ELG targets, exposure times) will follow from detailed R&D and science trade studies.

2.B Weak Lensing and Redshift Space Distortions

DESpec spectroscopy would enable measurement of galaxy clustering in redshift space. A galaxy's redshift is the combination of its Hubble flow motion and the radial component of its peculiar velocity due to nearby structures. Clustering in redshift space is therefore distorted

Draft. Do not circulate

(anisotropic) relative to clustering in real space, due to the effects of peculiar velocities. In linear perturbation theory and assuming linear bias between galaxies and dark matter, the galaxy density perturbation Fourier amplitude in redshift space is given by (Kaiser 1987)

$$\delta_g^s(\mathbf{k}) = (b + f\mu^2)\delta(\mathbf{k})$$

where b is the linear bias factor for the given population of galaxies, f is the linear growth factor defined above, μ is the cosine of the angle between **k** and the line of sight (*not* the same μ as in Sec. 2.A), and $\delta(\mathbf{k})$ is the real-space dark matter perturbation Fourier amplitude. Measurement of the anisotropy (μ-dependence) of the galaxy power spectrum in redshift space thus provides a measure of the growth rate of fluctuations, *f(a),* which in turn is sensitive to the properties of dark energy.

Figure 2.1 (from Gazatanaga, et al. 2011) shows a first estimate of the 68% CL statistical constraints on w_0, w_a, and γ that would be expected with a baseline 5000 sq. deg. DESpec survey from redshift space distortions alone (RSD, purple), from DES weak lensing alone (Shear, blue), from the combination of RSD and weak lensing in non-coincident parts of the sky (red, RSD+Shear, e.g., from BigBOSS+DES), and from the coincident combination of RSD+WL (yellow, i.e., DESpec+DES). It is found that the combination of weak lensing and RSD measurements in the same spatial volume (yellow), as DESpec plus DES would provide, leads to stronger constraints on dark energy and modified gravity (Bernstein & Cai 2011, Cai & Bernstein 2011, Gaztanaga, et al. 2011). In this calculation, the DESpec survey is assumed to obtain redshifts for 1000 galaxies per sq. deg. to limiting magnitude of i_{AB}=22.5, with a mean redshift of about 0.6. RSD×WL (DES+DESpec) improves the (marginalized over γ) DETF FoM for w_0, w_a by a factor of about 4.6 compared to DES weak lensing. The spatial overlap of RSD spectroscopy with WL photometry is found to improve the DETF FoM compared to non-overlapping surveys. We should caution that the FoM gains depend on the detailed assumptions of the calculations, particularly which DE probes are included in the mix and he assumptions made about the respective photometric and spectroscopic surveys (Bernstein & Cai 2011, Cai & Bernstein 2011).

Draft. Do not circulate

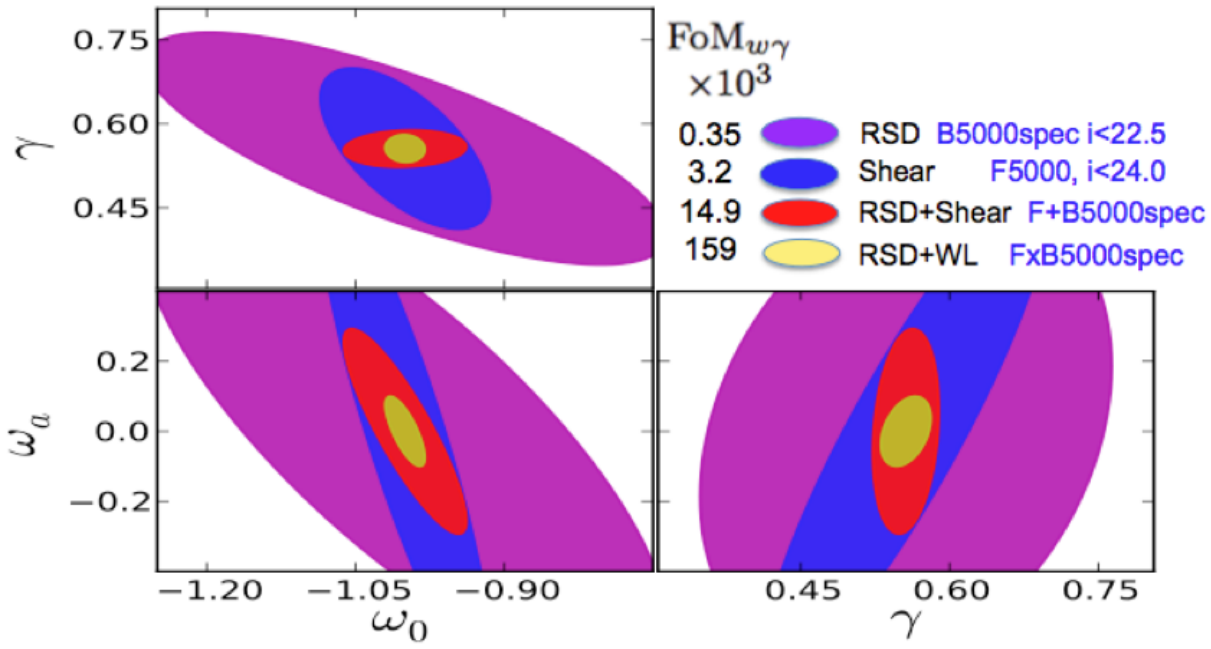

Figure 2.1: Forecast 68% CL constraints on dark energy (w_0, w_a) and structure growth (γ) parameters from DES weak lensing alone (blue), redshift space distortions alone (purple), the combination of the two without spatial overlap (red) and with spatial overlap (yellow, i.e., DES+DESpec). The lensing measurements include shear-shear, galaxy-shear, and galaxy-magnification correlations. Each two-parameter combination is marginalized over the third parameter. From Gaztanaga, et al. (2011).

The RSD measurements to constrain the growth of structure put a premium on measurements at relatively modest redshift, z~0.5-1, and on measuring redshifts for the most massive halos, i.e., those hosting groups and clusters (Bernstein & Cai 2011). This suggests that Luminous Red Galaxies at intermediate redshifts would be ideal targets.

2.C Large-scale Structure and Baryon Acoustic Oscillations

The large-scale clustering of galaxies contains a feature at ~110 h^{-1} Mpc, detectable as a slight enhancement in the two-point correlation function on that scale or as periodic wiggles in the power spectrum. This scale is set by the sound horizon, the distance that acoustic waves in the photon-baryon plasma travelled by the time that ionized hydrogen recombined 380,000 years after the Big Bang. This BAO feature is imprinted dramatically on the cosmic microwave background anisotropy as a characteristic angular scale of ~1 deg in the size of hot and cold spots in the CMB temperature map. It is a more subtle feature in the galaxy distribution, since structure formation is driven primarily by gravitational instability of dark matter. First detected in the distribution of LRGs in the SDSS redshift survey (Eisenstein, et al. 2005), its measurement is the primary aim of the on-going SDSS-III Baryon Oscillation Spectroscopic Survey (BOSS),

Draft: Do not C

which is targeting 1.5 million LRGs over 10,000 sq. deg. to redshift z~0.6. A number of next-generation BAO-centric redshift surveys are under construction (e.g., HETDEX) or have been proposed (e.g., BigBOSS, WEAVE, VXMS, SUMIRE, EUCLID, WFIRST). The BAO feature is useful for dark energy studies, because it acts as a standard ruler (e.g., Blake & Glazebrook 2003, Seo & Eisenstein 2003). Photometric surveys such as DES and LSST will probe the BAO feature in angular galaxy clustering, measuring the angular diameter distance $D_A(z)$ and thereby constraining the expansion history. Redshift surveys improve the accuracy on $D_A(z)$ and, in addition, measure BAO in the radial direction, which provides a direct measure of *H(z)*. Greater precision in these geometric measures over a range of redshifts translates into greater precision in the dark energy equation of state.

The SDSS LRG BAO measurement constrained *H(z)* and $D_A(z)$ to ~4 and 1.6% precision at redshift z~0.35. BOSS is expected to determine these over a range of redshifts up to z=0.6, with its best precision of ~2 and ~1% at the upper end of that range. DES will probe $D_A(z)$ via angular BAO with a precision of about 2.5% but over a larger redshift range, to z~1.3. A DESpec survey that targets Emission Line Galaxies to z~1.5 over 5000 sq. deg. would reach a statistical precision of ~2.5% in *H(z)* and 1.5% in $D_A(z)$ at z~0.9 but with useful measurements over the entire redshift range. Extending the DESpec ELG survey to 15,000 sq. deg. by targeting LSST galaxies in addition would improve the precision on H and D_A to about 1.5 and better than 1%; this precision would be achieved by BigBOSS as well. Combining DESpec and BigBOSS BAO would be expected to further improve each of these constraints by ~40%.

In designing a BAO survey, the precision of the H and D_A measurements (and therefore of the DE constraints) is set by the relative statistical uncertainty in measuring the large-scale galaxy power spectrum, $\sigma(P)/P \propto V_{eff}^{-1/2}$, where V_{eff} is the effective volume of the survey,

$$V_{eff} = \left(\frac{nP}{nP+1} \right)^2 V_{survey} \ ,$$

V_{survey} is the survey volume, and n is the survey galaxy number density. To minimize cosmic variance errors, the survey should cover large volume V_{survey}; to minimize the impact of Poisson errors, the galaxy sampling density should satisfy $nP \geq 2-3$. To reach large effective volume, we wish to select galaxies with adequate sampling density out to high redshifts, z~1.5, which leads one to preferentially target Emission Line Galaxies (ELGs), as described in Sec. 3. Given the ELG large-scale power spectrum amplitude, the desired number density is very roughly n> 3×10^{-4} h^3 Mpc^{-3}; for a 5000 sq. deg. survey to that redshift, the survey volume is of order 2×10^{10} h^{-3} Mpc^3, which implies an approximate total of $N=nV_{survey}$~6 million ELG redshifts, with an areal density of 1200 per sq. deg. This figure sets the survey design of Sec. 3. For a wider-area BAO survey that also targets LSST galaxies, one would seek to maintain the same target density, resulting in ~18 million ELG redshifts over 15,000 sq. deg.

Draft: Do not circulate

2.D Galaxy Clusters

DES will measure the abundance of massive galaxy clusters to redshift $z\sim1.3$ and use it to probe DE. The abundance of dark matter halos with mass and redshift, $dN(M,z)/dzd\Omega$, is sensitive to DE through the expansion history, which determines the volume element, and to the growth rate of structure, which determines the intrinsic halo density as a function of time. In this technique, clusters serve as proxies for massive dark matter halos. DES will determine cluster redshifts photometrically with sufficient precision for this test. However, since the masses of dark matter halos are not directly observable, this technique relies critically on the ability to determine the relation between cluster observables (such as the number of red galaxies above a certain luminosity) and the underlying halo masses; in particular, the mean and scatter of the mass-observable relation must be determined either internally (e.g., via self-calibration or weak lensing) or externally, by performing other measurements that constrain the relation. Clearly, external measurements that help reduce the uncertainty in the cluster mass-observable relation will strengthen the resulting DE constraints (Cunha 2009, Wu, Rozo, & Wechsler 2010). DESpec can provide such external information for DES clusters by providing dynamical cluster mass estimates: measuring redshifts for several tens of galaxies in a cluster provides an estimate of its velocity dispersion and therefore of its mass. Well-designed spectroscopic follow-up could improve the DES cluster DE FOM by a factor of several even if carried out over a subset of DES clusters. Targeting for this sample would synergize with the LRG targeting for RSD and BAO studies but would likely require additional cluster-optimized exposures as well.

2.E Supernovae

The DES Supernova Survey will measure high-quality light curves for ~4000 type Ia supernovae to redshifts $z\sim1$ through repeat imaging of a 30 sq. deg. region over the course of the survey. Given limited spectroscopic resources, only a fraction of those will have follow-up spectroscopy while the supernovae are bright enough to detect. For the rest, follow-up spectroscopy of the host galaxies will be needed to precisely determine the SN redshift, which is important for increasing the precision of the SN Hubble diagram and reducing contamination from non-Ia SN types. The spectroscopic measurement of SN Ia host-galaxy properties (star-formation rates, gas-phase metallicities, etc) has become even more important with the results of recent studies (Kelly et al. 2010, Lampeitl et al. 2010, Sullivan et al. 2010, Gupta et al. 2011, D'Andrea et al. 2011) indicating that SN Ia luminosities (and therefore distance estimates) are correlated with host-galaxy properties. This correlation must now be taken into account in order to control SN cosmology systematic errors due to evolution of the mix of host-galaxy types (Sullivan, et al. 2011). DESpec could contribute to this program by measuring host-galaxy spectra of ~30% of the DES SN Ia sample.

Draft: Do not circulate

2.F Photometric Redshift Calibration

All four DE probes in DES rely on accurate estimation of galaxy photometric redshifts using color and other information from the DECam grizY images. The DES survey strategy is designed to optimize galaxy photo-z measurements to redshifts $z>1$, and the synergy of DES with the near-infrared (JHK) ESO Vista Hemisphere Survey will improve the photo-z precision of the survey. The weak lensing and galaxy clustering measurements in DES in particular rely on accurate estimation of the galaxy redshift distribution, *N(z),* and therefore require accurate estimation of the photo-*z* error distribution (variance and bias) as a function of redshift. Uncertainties in the variance and bias of the photo-z estimates lead to systematic errors that degrade DE constraints (Huterer et al. 2005, Ma, Hu, & Huterer 2006).

Determining the error distribution as well as training empirical photo-*z* estimators requires spectroscopic samples of $\sim 10^4$-10^5 galaxies that cover the range of galaxy properties (colors, redshifts, flux limits, etc) of the photometric sample. While such spectroscopic samples in the DES survey footprint exist to approximately the DES depth, they are incomplete at the faintest magnitudes DES will reach.

The DESpec survey could aid in DES photometric redshift calibration in two ways. First, it will provide a large number of additional redshifts for training, validation, and error estimation for empirical photo-z methods, although not to the flux limit of the DES. Second, such a large sample of galaxy redshifts extending over the entire DES footprint can in principle enable new methods that can augment traditional photo-z estimates at faint magnitudes. In particular, since galaxies are clustered, a faint galaxy in the DES photometric survey that is near on the sky to a brighter galaxy with a DESpec redshift will have a reasonable probability of having the same redshift as the spectroscopic galaxy (Newman 2008, Matthews & Newman 2010). The DESpec redshifts therefore act as informative redshift priors for neighboring DES galaxies; the utility of this approach for DE photometric surveys is under active study (e.g., Bernstein & Huterer 2010).

3. Survey Definition and Requirements

The scientific goals of the DESpec spectroscopic survey lead to a survey definition that acquires at least 1000 galaxy redshifts per square degree up to $z\sim1.5$ over at least the DES footprint of 5000 square degrees. The area may be extended up to 15,000 square degrees by later using LSST photometry for spectroscopic target selection. The DES and LSST photometry (together with VISTA JHK photometry) yields not only fluxes and photometric redshifts but also galaxy image shapes and surface brightnesses. All of this information can be exploited to select a sample of galaxies that satisfy the joint requirements of large redshift range, adequate volume sampling, and control over any bias introduced due to sample selection or redshift failures. In practice, we expect to use galaxy flux, color (and photo-z), and surface-brightness to sculpt the redshift distribution of the survey. We plan to target a mix of emission-line galaxies (ELGs)---which predominate at high redshift and which yield efficient redshift estimates to $z\sim1.7$ based upon

Draft. Do not circulate

their prominent emission lines---and luminous red galaxies (LRGs), which have brighter continuum spectra and higher clustering amplitude and that offer good redshift success rates up to z~1. The target selection will ultimately be chosen to optimize the science yield; at this stage, we present some examples of survey selection to demonstrate the feasibility of the survey, to set the scale, and to derive constraints upon the instrument design.

3.A Simulated Galaxy Catalogs

We have created simulated catalogs of galaxies to quantify the yield of a particular spectroscopic selection scheme, to predict the number of potential targets, and to compute the sensitivities and thereby the rate of progress of the survey. The simulations are built directly from the observed COSMOS catalog of Capak et al. (2009) and Ilbert et al. (2009). We refer to this simulation as the COSMOS Mock Catalog (CMC) (Jouvel et al. 2009).

The COSMOS photometric-redshift catalog (Ilbert et al. 2009) was computed with 30 bands over 2 deg^2 (GALEX for the UV bands, Subaru for the optical (U to z), and CFHT, UKIRT, and Spitzer for the NIR bands). It achieves very good photo-z accuracy and low catastrophic redshift rates due to careful calibration with the spectroscopic samples zCOSMOS and MIPS. The CMC is restricted to the area fully covered by HST/ACS imaging, 1.24 deg^2 after removal of masked areas. There are a total of 538,000 simulated galaxies for i < 26.5 in the mock catalog, leading to a density of roughly 120 gal/arcmin^2. AGN, stars, and X-ray sources were removed from the input COSMOS catalog.

A photo-z and a best-fit template spectrum (including possible additional extinction) are assigned to each galaxy of the COSMOS catalog. We first integrate the best-fit template through the instrument filter transmission curves to produce simulated magnitudes in the instrument filter set. We then apply random errors to the simulated magnitudes based upon a simple magnitude-error relation in each filter. The simulated mix of galaxy populations is then, by construction, representative of a real galaxy survey, and additional quantities measured in COSMOS (such as galaxy size, UV luminosity, morphology, stellar masses, correlation in position) can be easily propagated to the simulated catalog. The COSMOS mock catalog is limited to the range of magnitude space where the COSMOS imaging is complete (i_{AB} ~ 26.2 for a 5 sigma detection, see Capak et al. (2007) and Capak et al. (2009)).

We assign emission-line fluxes to each galaxy of the CMC by modeling the emission-line fluxes (Ly alpha, [OII], H beta, [OIII], and H alpha) using the Kennicutt (1998) calibration. We first estimate the star-formation rate (SFR) from the dust-corrected UV rest-frame luminosity already measured for each COSMOS galaxy. The SFR can then be translated to an [OII] emission-line flux using another calibration from Kennicutt (1998). The relation found between the [OII] fluxes and the UV luminosity is in good agreement with the VVDS data and is valid for different galaxy populations. For the other emission lines, we adopt intrinsic, unextincted flux ratios of [OIII]/[OII] = 0.36; H beta/[OII] = 0.28; H alpha/[OII] = 1.77 and Ly alpha/[OII] = 2 (McCall et

Draft. Do not circulate

al. 1985; Moustakas and Kennicutt 2006; Mouhcine et al. 2005; Kennicutt 1998).

The CMC does an excellent job of reproducing the counts and color distributions of galaxies observed in bands from 0.4 to 2.2 microns, for example comparing to the GOODS (Giavalisco et al. 2004) and UDF (Coe et al. 2006) surveys. The CMC also provides an excellent match to the redshift-magnitude and redshift-color distributions for I<24 galaxies in the VVDS spectroscopic redshift survey (Le Fèvre et al. 2005). For more detail about the CMC and its validation, see Jouvel et al. (2009).

3.B Spectroscopic Sensitivity

To compute the sensitivities (exposure time required to obtain a certain S/N for a particular simulated galaxy spectrum, and redshift success rates), we start with input spectra from the DES galaxy catalog simulations (provided by R. Wechsler & M. Busha) or from the COSMOS Mock Catalog (CMC, Jouvel et al. 2009), both of which model the detailed properties of the galaxy population at magnitudes and redshifts appropriate to DESpec. The DES catalog simulations provide galaxy spectra based upon the template models generated by the Kcorrect package (Blanton & Roweis 2007), while as just described the CMC provides spectra based on the COSMOS data, providing in particular detailed distributions of line fluxes for emission-line galaxies. We account for the transmission as a function of wavelength for the atmosphere.

For this initial study, we have simply assumed that the DESpec system has 50% of the net throughput of DECam. We also account for the fraction of galaxy light entering a fiber, using either an analytic Gaussian model and the galaxy size distribution from the CMC or the detailed DES galaxy image simulations. The dominant source of noise for the DESpec spectra comes from the night sky, which we model using the high-S/N, high-resolution spectral atlas of Hanuschik (2003) plus the extensive spectroscopic archives from the SDSS and BOSS surveys. We take care to use data with resolution similar to or better than DESpec, in order to properly sample the much lower sky continuum levels in between the forest of atmospheric airglow emission lines in the red.

Draft. Do not circulate

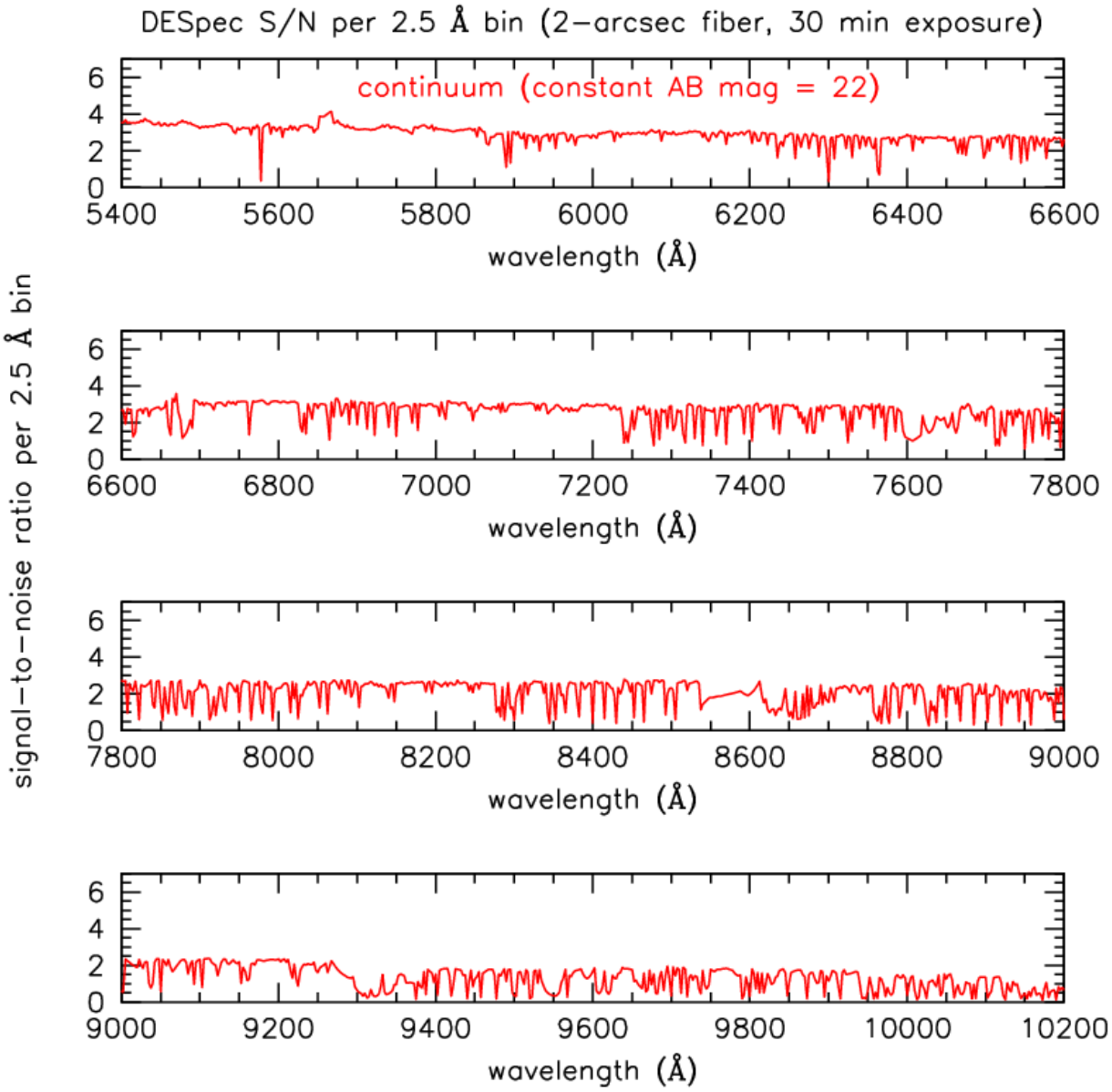

Figure 3.1: The signal-to-noise ratio in 2.5 A bins as a function of wavelength for an input spectrum with m_{AB} = 22 and an exposure of 30 minutes. The basis of the calculation assumes the DESpec throughput and the sky noise as described in the text.

Draft

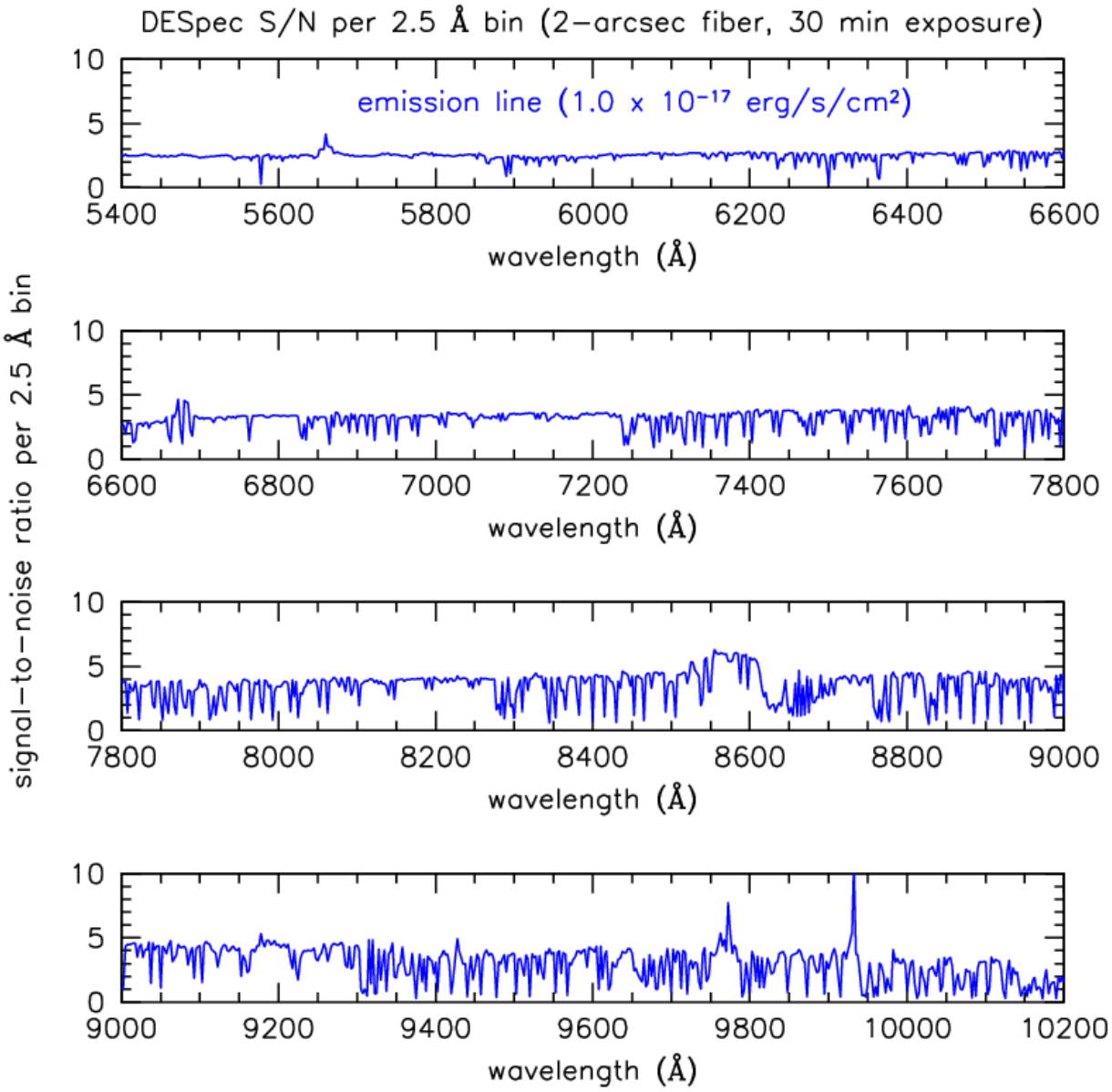

Figure 3.2: Same as Fig. 3.1 except that the signal is an unresolved emission line with flux 10^{-17} erg/sec/cm^2.

The above components are implemented in a simulation package written in IDL, which generates flux-calibrated, one-dimensional extracted spectra with the signal and noise properties and wavelength resolution appropriate to DESpec. The simulated DESpec spectra are then used to calculate S/N and redshift success rates as functions of different galaxy properties, in particular galaxy magnitude, redshift, and emission-line strength. For emission-line galaxies, we make measurements of the S/N of the emission-line flux, especially of the [OII] 3727 line that will be the most useful for redshift determination at z>0.5. In addition, we use the standard redshift measurement technique of cross-correlation with template spectra, as implemented in the IRAF

Draft

external package rvsao (Kurtz & Mink 1998), to compare measured vs. true redshifts and to estimate the fraction of successful redshift measurements vs. galaxy properties. This will be useful for absorption-line galaxies, for which redshift measurement will be based upon spectral features spread over a range of wavelengths rather than on individual strong emission lines. We plot two examples of DESpec signal-to-noise calculations, one for a hypothetical object that has a continuum level with constant AB mag = 22 (Fig. 3.1) and one for an emission line with flux = 1.0×10^{-17} erg/s/cm^2 (Fig. 3.2). In both cases we assume a 2-arcsec-diameter fiber, 70% of the light entering the fiber, a 30-minute exposure time, airmass 1.3, and the sky from Hanuschik (2003) as appropriate for dark time. We plot the S/N in fixed bins of 2.5 A˚, taken to be the wavelength resolution element, corresponding to a spectral resolution R=3500 at about 900 nm. For the emission line we assume the case of a narrow line whose flux is entirely contained within a single resolution element. As noted in Section 4, the results are not very sensitive to the assumed fiber diameter.

3.C Luminous Red Galaxy Selection

For galaxy clustering measurements for BAO and RSD, LRGs are convenient because they occupy dense regions and are thus strongly biased relative to the dark matter, b~2, so the clustering amplitude is high. With our simulations we have estimated the completeness rate for objects in the CMC catalogue. We plot in Fig. 3.3 a preliminary example of the redshift completeness for LRGs, showing the magnitude, as a function of redshift, where the DESpec redshift success rate is expected to be 90%. Also shown is the apparent magnitude vs. redshift relation for an LRG with luminosity of 3L* (Eisenstein et al. 2001), showing that the survey is expected to be about 90% efficient for bright (>3L*) LRG redshift measurement out to z = 1.3 in a 30 minute exposure, modulo target selection efficiency, fiber collisions, etc.

Using DES+VHS imaging, LRGs can be selected to yield a relatively flat redshift distribution over the range $0.5 < z < 1$ by using selection cuts in r-z vs. z-H color space. We plot these color diagrams in Figure 3.4. These cuts supply more than the needed density of LRG targets, so the targets can be randomly sampled. The galaxies yielded by Cut I amount to 770 galaxies per square degree at magnitudes in the z band brighter than 21. For Cuts II and III we have ~60 objects per square degree at magnitudes brighter than 22 in the z band, but they are at significantly higher redshifts.

Draft. Do not circulate

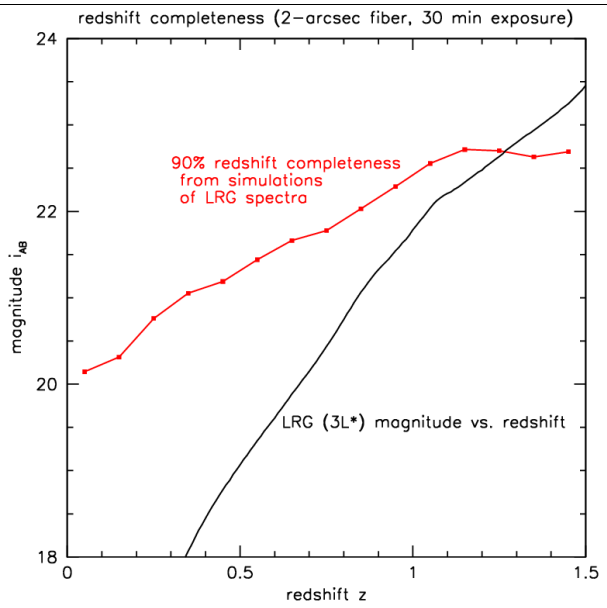

Figure 3.3: The red points and curve indicate the i_{AB} magnitude vs. redshift where the redshift success rate for an LRG spectrum is 90%, based on our spectroscopic simulations. Black curve shows the magnitude vs. redshift relation for an LRG with L= 3L* (Eisenstein et al. 2001), showing that DESpec should be 90% successful for bright LRG redshift measurements out to z = 1.3 in a 30 minute exposure.

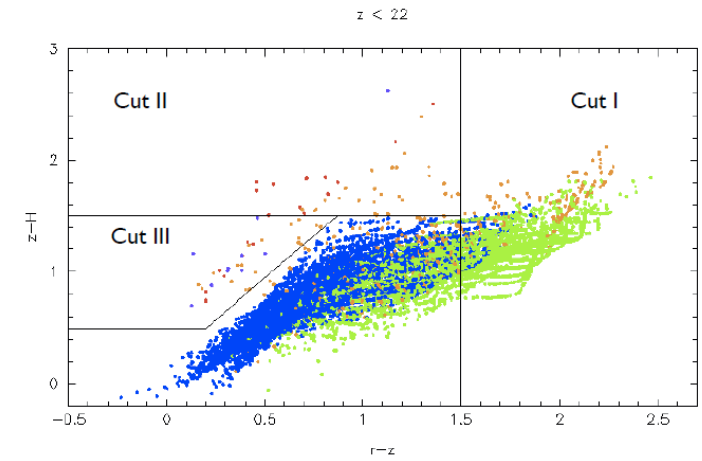

Figure 3.4: Illustration of targeting efficiency of *z-H* vs. *r-z* color-color cuts I, II, and III for galaxies with *z*-mag <22: for redshift z<0.5 (blue), 0.5<z<1.1 (green), and z>1.1 (gold). Red and purple are successively higher redshift bins.

3.D Emission-line Galaxy Selection at High Redshift

Here we describe simulations to investigate selection criteria for a survey targeting emission-line galaxies at redshifts higher than accessible with luminous red galaxies for BAO and RSD studies. Using the CMC (Jouvel et al. 2009), we assume that the survey would reach the line sensitivities described earlier, namely a signal-to-noise ratio of around 5 for fluxes larger than 3×10^{-17} erg/s/cm^2 from wavelengths 600 to 1000 nm (Fig. 3.2). This is reached for a 30 min exposure, which we take as the baseline.

We can use photometric redshifts to select high-redshift galaxies. Fig. 3.5 (left panel) shows the redshift distribution of emission-line galaxies that would be obtained with DESpec with a photometric redshift cut between 1< z_{phot} < 2, i-magnitude<23, and a S/N=5 detection of one of various lines: OII line (blue), Hα (red), OIIIa (magenta), OIIIb (brown), or Hβ (gold). (Color-color instead of photo-z selection, similar to that of the DEEP2 redshift survey of ELGs over the

Draft. Do not circulate

redshift range 0.7 to 1.4, gives a similar result.) Exercises such as this give a first indication of the spectroscopic success rates, redshift distribution, and numbers of galaxies that would result from such a survey. A wavelength range 600–1000 nm allows Hα to be detected up to z=0.52 and [OII] to be detected at z>0.6; the upper limit in redshift for [OII] is z=1.7. We reach a total number of 2500 galaxies/deg^2 between redshift 1 and 1.7 for galaxies with i<23. Redshift measurements coming from lines other than [OII] provide an additional 300 gal/deg^2 in this redshift range.

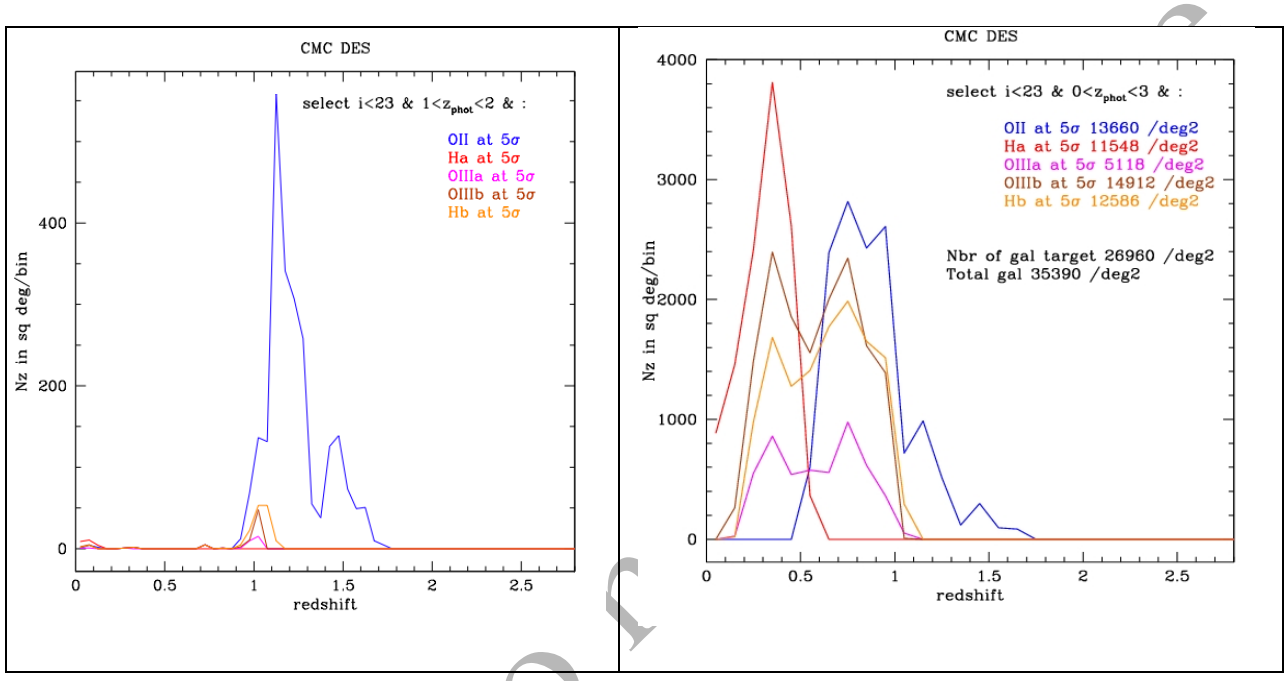

Figure 3.5: Example of the yield of a particular ELG target-selection scheme based on the COSMOS Mock Catalog (CMC) simulations, assuming 5-sigma line detections as expected for a 30-minute DESpec exposure. Galaxies brighter than i=23 are selected that have photometric redshifts between 1 and 2 (left); the distribution of those satisfying a much broader photometric redshift cut between 0 and 3 are shown in the right panel. This shows that selection of high-redshift sources via photometric redshift is effective, and it shows that, as expected, [OII] is the principal spectroscopic feature in this range of redshifts. Furthermore other redshifts can be accessible with other lines, including Hα, Hβ, and OIII.

In Figure 3.6 we show photometric vs. true redshift for the same flux-limited sample of galaxies. This allows us to estimate the galaxies we miss due to the photo-z selection. For galaxies selected with photometric redshifts 1 and 2, 4.5% of the galaxies will have true redshifts outside the desired redshift range of 1-2. If we choose instead to select a low-redshift emission-line sample (photo-z's between 0.5 and 1), 12% of the target galaxies will have true redshifts outside the selection range. This study indicates that DES+VHS imaging can yield high-efficiency target selection of high-redshift galaxies based on photometric redshift cuts.

Draft. Do

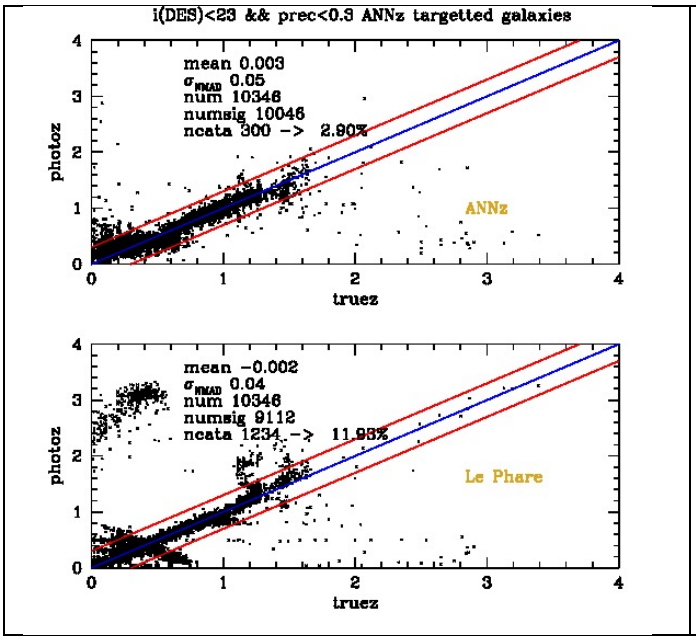

Figure 3.6: Example of the yield of a particular target-selection scheme based on the COSMOS Mock Catalog (CMC) simulations. If photo-z selection is applied, we can select galaxies at high redshift (z=1-2) with 95.5% success and galaxies at intermediate redshift (between 0.5 and 1) with 88% success rate. DES+VHS photometry assumed. Upper panel: ANNz photo-z estimator; lower panel: Le Phare estimator.

Using broadband photometry, an efficient targeting strategy can be realised using a neural network technique such as ANNz (Collister & Lahav 2004). Indeed, Abdalla et al. (2008) showed that there is some predictability of emission line strength from galaxy colors. Using the CMC catalog in the DES+VISTA bands, we show in Fig 3.7 that we can select strong emission line galaxies.

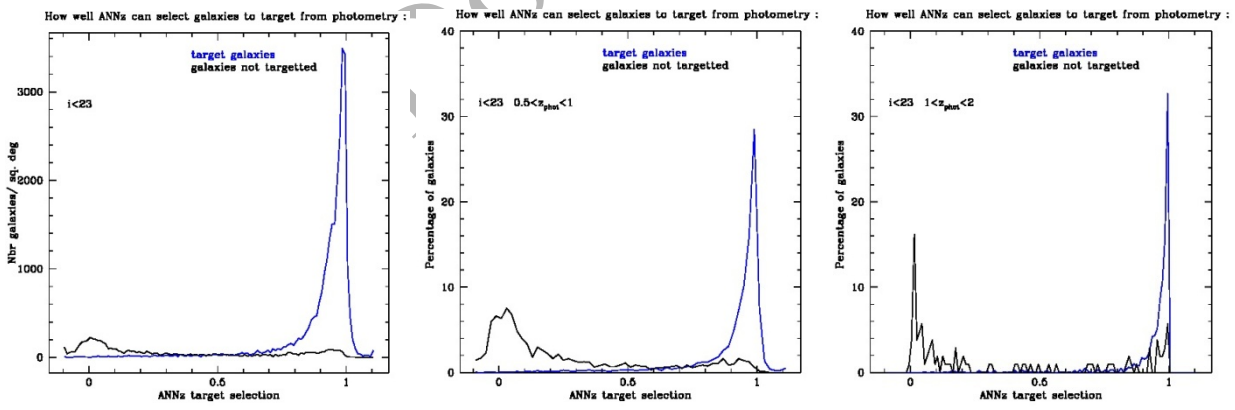

Figure 3.7: the number of galaxies per square degree as a function of ANNz target selection value. The blue line corresponds to galaxies for which we will be able to measure a redshift, the "target galaxies:" they have at least one emission line detected at 5 sigma using DESpec and we assign them a value of 1. The black line corresponds to galaxies that do not have a strong emission line detectable; we assign them a value of 0.

Do not circulate

Using 10,000 galaxies as a training sample, we derive ANNz target selection values. To define a selection criterion from the ANNz values, we draw the cumulative number of galaxies per square degree as shown in Fig 3.5. A criterion of 0.8 selects most of the emission-line galaxies and has small contamination from weak-emission-line galaxies. We then derive the Spectroscopic Success Rate (SSR) as the percentage of galaxies for which we will be able to measure a redshift, as shown in Figs 3.8 and 3.9. The dotted lines in Fig. 3.9 represent the SSR for different magnitude cuts, while the solid lines represent the percentage of galaxies compared to the total number of galaxies at the magnitude cut.

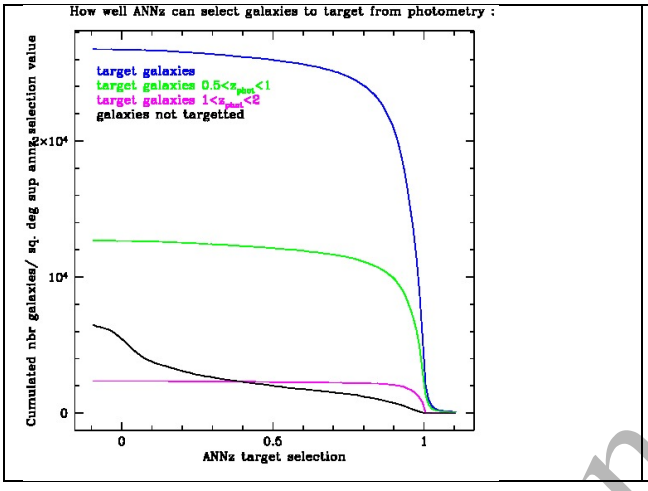

Figure 3.8: Cumulative number of galaxies/deg^2 as a function of the ANNz target selection value for the target galaxies in blue, the target galaxies with a photometric redshift between [0.5-1] in green and [1-2] in magenta, and the galaxies not targeted in black. Using a ANNz target criterion of 0.8, we are able to reach a SSR of 95% at i<23 AB mag targeting close to 75% of all the galaxies at i<23. We will have a yield of 24000 galaxies/deg^2.

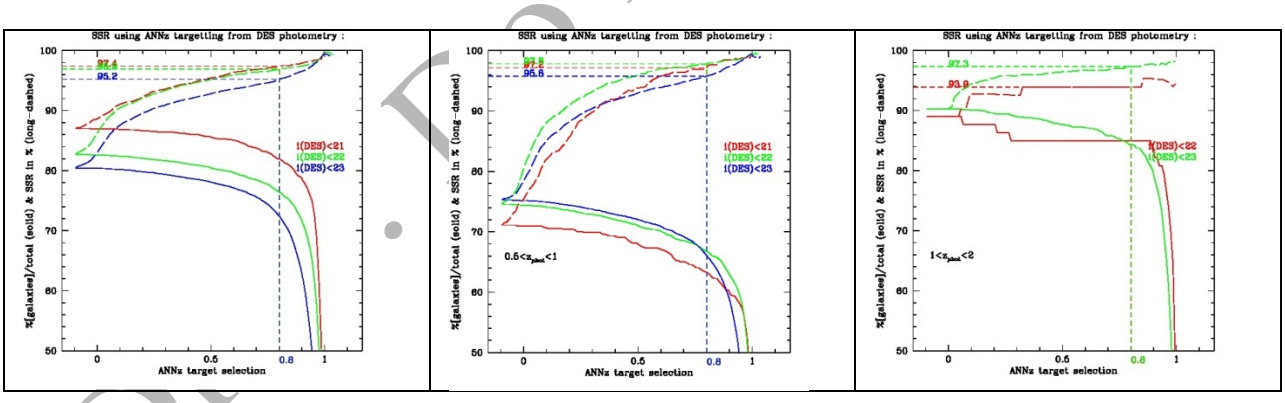

Figure 3.9: Spectroscopic Success Rate (dashed lines) and cumulative number of galaxies (solid lines) as a function of ANNz target selection values for magnitude i<23 in blue, i<22 in green, and i<21 in red. The left figure represents all the galaxies meeting the different magnitude cuts, the middle figure represents the galaxies for which 0.5 <z_{phot}< 1, and the right figure 1< z_{phot} < 2.

Draft. Do not circulate

3.E Survey Strategy

This section gives the outline of how the survey might acquire the spectra. The constraints are the field of view of the focal plane (2.2 degrees in diameter), the number of fibers (~4000), and the total survey time available in allocated nights, *N*, which is to be determined. For this exercise, we assume 80% of the allocated nights are astronomically useable and an average of 7.7 hours on the sky per useable night, both based on historical CTIO weather data.

If the DESpec fibers span the full instrument circular FOV of 3.8 sq. deg. (as in Fig. 4.4 below), one could cover the 5000 sq. deg. DES footprint with, e.g., 1667 circular tiles, with 27% of the area covered by two tiles, similar to what was done for the SDSS spectroscopic survey. This would enable one in principle to place more fibers in dense regions of large-scale structure or to reach longer cumulative exposures on objects in the overlap regions; in this case, for 4000 fibers, the fiber density per tile on the sky is 1050 targets per sq. deg, and the fiber pitch is 6.8 mm.

This surface density of fibers per tile is comparable to the desired surface density of successful galaxy targets for BAO and RSD studies to redshift $z \sim 1.7$ (Secs. 2.B and 2.C). As an example, let us assume 65% combined targeting and redshift success rate for 900 flux- and photo-z selected ELG targets per sq. deg. and 80% efficiency for 120 LRG targets per sq. deg. for 30-minute cumulative exposures per target, with a small number of fibers left for sky background or other science targets per tile. In two tilings (30 min exposure for each tile) per 3.8 sq. deg. field, we would obtain redshifts for ~7 million galaxies (~5.8 M ELGs and ~1 M LRGs) over 5000 sq. deg. in about 300 allocated nights, allowing for 10% overhead. With, e.g., 15-minute individual exposures, this strategy would also provide some flexibility to adjust the target list over time, according to which galaxies had already achieved sufficient signal-to-noise ratio to yield a redshift. Since the source list of targets will be high (there are of order 10,000 galaxies per square degree brighter than $i = 22.5$), this approach can also help accommodate tile-to-tile fluctuations due to large-scale structure. For example, in underdense regions, additional galaxies can be added that comprise a different complete sample, and in overdense regions, having multiple visits per tile will help to achieve the required completeness (or calibrate the incompleteness). Exposing for one hour (cumulative) per 3.8 sq. deg. field in this manner, one could cover 15,000 sq. deg. (the bulk of the extragalactic sky for LSST) with ~20 million redshifts in ~900 allocated nights. These numbers are all approximate and require more detailed simulations to refine.

Using colors, surface brightness, and image shapes, the redshift and type of galaxy selected for spectroscopy can be tuned to the scientific priorities (e.g., BAO, redshift-space distortions, legacy). The large reservoir of potential targets provides considerable latitude in designing the survey strategy.

Draft. Do not circulate

4. DESpec Instrument Definition

DESpec would be a multi-fiber spectrometer that uses the same mechanical structure and most of the same corrector optics as DECam, thereby achieving a substantial cost savings compared to an ab-initio instrument. The instrument could consist of 7-10 single-arm optical-fiber spectrographs fed by a robotic, multi-fiber positioner at the prime focus of the CTIO 4m. In its initial design, DESpec would operate over the wavelength range 600-1000 nm, have a spectral resolution R(1000 nm)~3330, and be able to observe 4000 targets simultaneously. The 20 2kx4k CCDs (2 per spectrograph) and the CCD readout would be identical to those used for DECam. DESpec would be interchangeable with DECam in a reasonably short time.

An alternate spectrograph design has been developed that uses 2-arm spectrographs and supplies increased wavelength coverage, operating from 500-1050 nm. This alternate design uses the same optical corrector and fiber positioner as the design outlined above. Variants of this design also include the capability for increased resolution in the red side compared to the single-arm spectrographs as well as the option to eliminate the atmospheric dispersion compensator. More detailed descriptions of each design are presented below.

4.1 DESpec Optical Corrector Design

The DECam optical corrector was designed to make excellent images in individual filter bandpasses, but refocus was allowed, and lateral chromatic aberrations were controlled only within each bandpass. The 5-element DECam corrector optics produces a flat focal plane with a clear aperture radius of 225.54 mm. It has an f/2.9 beam that has 3.8 degrees of non-telecentricity at the edge of the focal plane. It also uses a filter-changer with 13 mm-thick filters. The DECam lenses are called “C1” (the largest, furthest from the focal plane) through “C5”. C5 is the final DECam optical element and is also the imager Dewar window, so it travels with DECam when it is removed from the telescope. C1 through C4 would remain in the prime focus cage during an instrument swap of DECam with DESpec. As of this writing (January 2012), the assembled and aligned DECam corrector optics are on-site at CTIO and ready for installation on the telescope.

Draft. Do not circulate

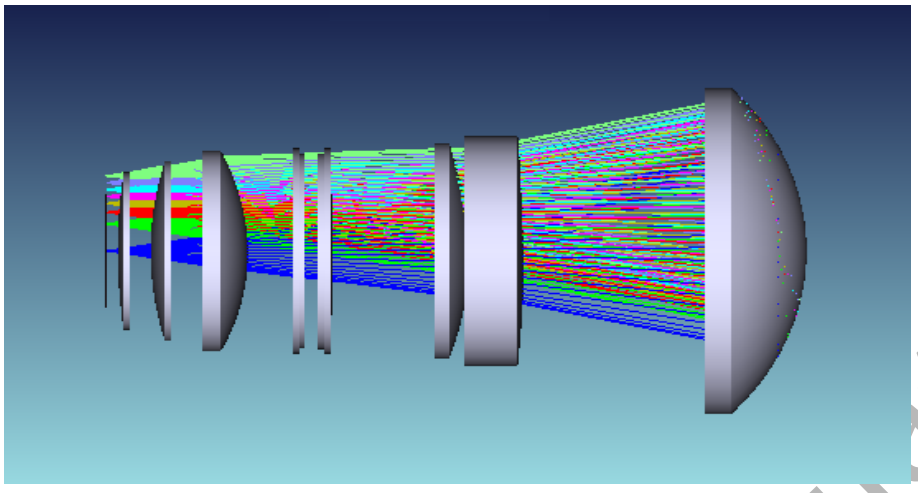

Figure 4.1: One option (DESpec-SK-3C) for the DESpec optics. From right to left they are C1 to C3, the two-component ADC, C4, C5', and the field-flattener C6. The focal plane of fiber-ends would be just to the left of the new C6. "C1" is a little less than 1 meter in diameter. The optical train is 1.9 meters long. C1, C2, C3, and C4 will already be in place for DECam.

4.1.1 DESpec Optical Corrector

DECam was required to deliver images that were comparable to the median site seeing. For DESpec, images are required to fall within a fiber diameter that is optimized for maximal S/N ratio of faint galaxies along with a minimum required spectral resolution. While the requirements on image sizes are similar, the impact of degradation in image size is different in the two cases. For DECam, a degradation of image size results in an inability to detect the smallest and faintest galaxies. For DESpec, a degradation of image size results in a reduced S/N ratio, but one can compensate (within limits) by increased observing time. DECam placed no constraint on the telecentricity of the beam incident on the focal plane, and the incoming beam is tilted up to 4 degrees at the focal plane edge. For DESpec, the fibers are constrained to be perpendicular to the focal plane, and an inclined beam would cause focal ratio degradation at the exit of the fiber. Thus, the beam needs to be perpendicular to the focal plane (telecentric) at all locations.

In addition, the DESpec corrector is required to produce a good image (though not as good as DECam) over the entire useful wavelength range. DESpec will reuse the 1st four elements of the DECam optical corrector (C1-C4). As noted above, C5 as well as the DECam filters would not be used for DESpec. For observations at high zenith angles, an Atmospheric Dispersion Compensator (ADC) can compensate for the natural prismatic effect of chromatic refraction in the atmosphere. Because the maximum zenith angle of DESpec has not been finalized, we have developed options for corrector optics both with and without an ADC. Here we present the option with the ADC, and in the next subsection we describe the ADC.

The single C5 lens in DECam is replaced with a pair of lenses C5' and C6 in DESpec. Both are made of fused silica. Such a pair is needed in order to achieve proper focus and telecentricity

Draft. Do not circulate

simultaneously. One surface (the concave face of the new C5') is aspheric. By using an asphere, the image quality is significantly improved at the field edge, and the curvature of C5 can be significantly reduced. Both lenses are rather thin, and the presence of an asphere on one might be of some concern. The thinness is somewhat to compensate for the extra glass thickness introduced by the ADC. However, the spectroscopic corrector lens of the SDSS 2.5 m telescope is even thinner and has a more severe aspheric shape on its convex side, so fabrication is expected to be feasible.

The present default DESpec corrector design, "DESpec-SK-3C", is shown in Figure 4.1. The optics achieves good spot size for wavelengths 500 nm < λ < 1050 nm, as shown in Figure 4.2. The RMS spot radius is 0.25" at the center and 0.44" at the edge. The peak off-incidence ray (non-telecentricity) is at a 0.45 degree angle of incidence. The focal surface has a radius of curvature of 8047.2 mm. The focal ratio of the corrector, f/2.9, is in the optimal range for collecting light in an optical fiber (Ramsey 1988).

The DESpec corrector design without an ADC has a comparable, but slightly worse, spot size, plus chromatic refraction. To partially compensate for this, one could use a galaxy target's photo-z as the expected redshift and optimally position the fiber for the wavelength at which a corresponding emission line or absorption feature is expected. Such a strategy has its own drawbacks but represents a possible descoping option to reduce upfront costs.

Draft: Do not circulate

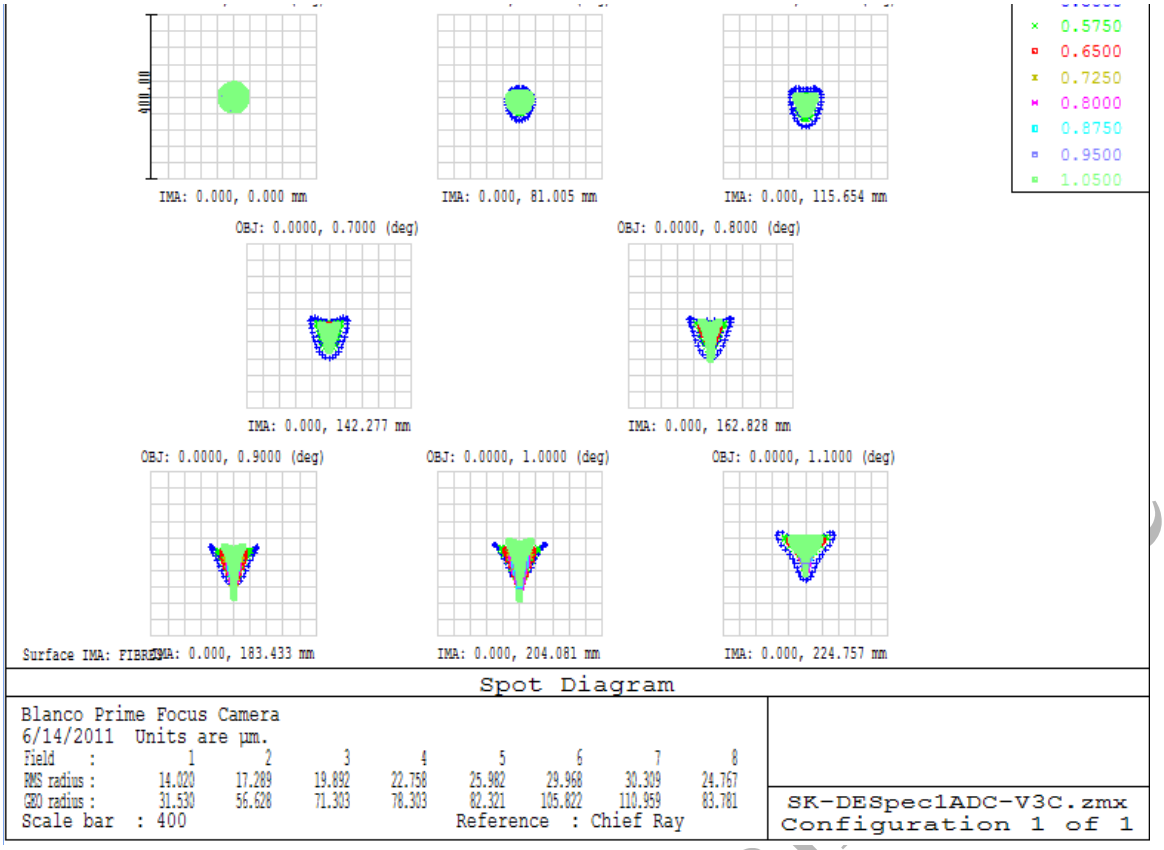

Figure 4.2: The spot size versus wavelength (0.5 (blue)–1.05 (green) microns) from the center of the focal surface (top-left) to the edge of the focal surface (radius of 1.1 deg, lower-right). The RMS spot radius is 0.26" at the center, 0.52" at the worst radius, and 0.44" at the edge. These results are from the "DESpec-SK-3C" design.

4.1.2 ADC Design

The atmospheric dispersion compensator is composed of a pair of crossed Amici prisms. Each prism is itself a double prism made of a crown and a flint glass with similar refractive indices. We have chosen N-BK7 and LLF1, since these glass types are typically selected for use in other large ADCs. By selecting the rotation angle of the crossed prisms, one can compensate for the dispersive effects of the atmosphere up to zenith angles of 60 degrees. The ADC designed for the WIYN One-Degree Imager (Muller, 2008) is similar in size and design to that which we expect for DESpec (see Figure 4.3). Optical studies show that improved images at the edge of the field can be obtained by making the first and last surfaces of the ADC mildly curved. Such an approach has been used for previous ADCs (e.g., the current Blanco prime focus corrector) and recent conversations with vendors indicate that they are not expected to be difficult to manufacture.

DESpec's ADC and shutter will fit into the large slot in the barrel that DECam uses for the filter-changer and the same shutter. There is sufficient room for an ADC in the DECam Barrel at the position of the filter-changer/shutter assembly, which is removable or installable in a short time. We do not need to use the filter changer while doing spectroscopy.

Draft. Do not c

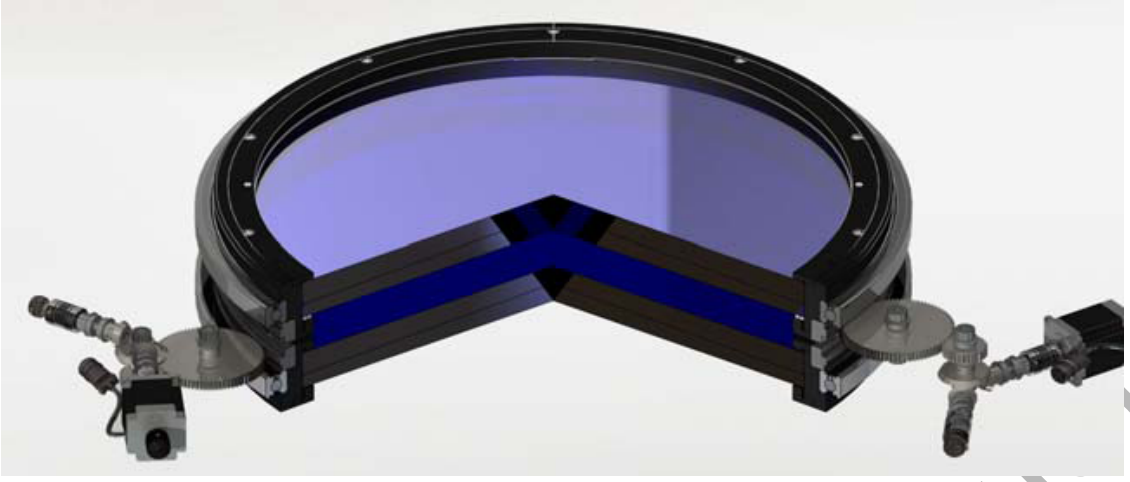

Figure 4.3: The WIYN One Degree Imager ADC is similar to that envisioned for DESpec. This ADC has a diameter of 635 mm. The prisms are rotated using a pair of encoded stepper motors.

4.1.3 R&D

Present R&D for the optics is aimed at understanding the optimal wavelength range for the science, optimizing the focal surface, and working out details and finalizing choices of materials for the ADC and the new elements at the focal plane. The ADC itself will be made from four elements that need to be glued together (or otherwise held) in pairs; this has to be done carefully, avoiding bubbles or other defects. A mechanism that performs the anti-co-rotation of the elements needs to be specified and designed.

4.2 The DESpec Fiber Positioner

The fiber positioner should be able to support ~4000 fibers at prime focus. The fiber positioner must move the tips of the optical fibers to predetermined positions for each exposure and then hold them in place for the length of the exposure. It must also gather the fibers into bundles that run to the spectrographs. Since DESpec will reutilize the corrector optics of DECam, the focal plane will be about the same size, i.e., a radius of 225.54 cm. This implies a separation between fibers (i.e., the pitch) of a bit less than 7 mm. Figure 4.4 shows the locations of 3781 fiber centers within the clear aperture radius using a 7 mm fiber pitch.

Draft. Do not circulate

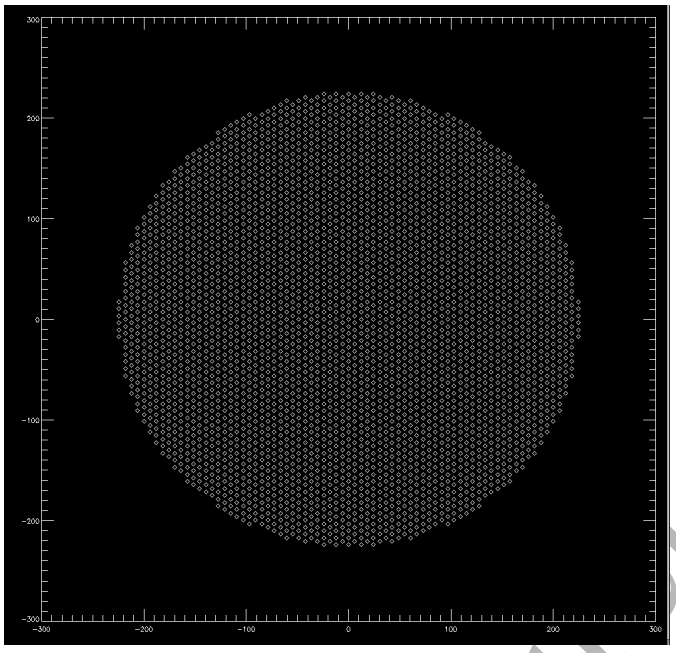

Figure 4.4: Array of DESpec fiber positioners. Here we show 3781 locations with 7 mm spacing (pitch) within the clear aperature. If the pitch were 6.3 mm, the clear aperture would accommodate 4675 fiber positioners. The x and y axes have units of mm's. Again, we use a clear aperture radius of 225.54 mm.

There are two general classes of fiber positioners that could provide technical solutions for DESpec: the "Twirling Post" design and the "Tilting Spine" design. Figure 4.5 shows a schematic (Seiffert, 2009) of the "Cobra" fiber positioner, under development at Caltech/JPL, that was considered for WFMOS and is being considered for the Subaru Prime Focus Spectrograph (Sumire). The fiber is held at the tip of the "twirling post". The post can rotate, and the tip can rotate with respect to the post, thus allowing the fiber to be positioned anywhere within a "patrol radius". A variant of this (phi-phi) design has a rotatable post with a tip that moves along the radius (r-phi).

Figure 4.6 shows a schematic (Akiyama, et al. 2008) of the second class, the "Echidna" fiber positioner developed at the Anglo Australian Observatory and currently used in the FMOS instrument on the Subaru Telescope in Hawaii. This "Tilting Spine" solution uses a unit positioner (Figure 4.7) that is tilted into place by a pair of piezo-electric motors at the base.

At present, the operating "Tilting Spine" type positioner (Echidna) has a smaller spacing between fibers (7 mm pitch) than the smallest operating "Twirling Posts" (WFMOS-Cobra prototypes, 12 mm). The patrol radius for the Echidna is equal to the pitch, and all six "nearest-neighbor" fibers can be positioned as close together as the size of the tip of the spine allows. The patrol radius for the prototype Twirling Posts is about 2/3 of the pitch and there are not so many nearest-neighbors. A scaled-up Echidna to DESpec size would have ~4000 fibers. The Cobra-type positioner would have 1000-1500 fibers with the present state-of-the-art; it is expected that

Draft: Do not circulate

they could be made with smaller pitch, which would increase the number of fibers, but there is more R&D required for this type of unit positioner than the other.

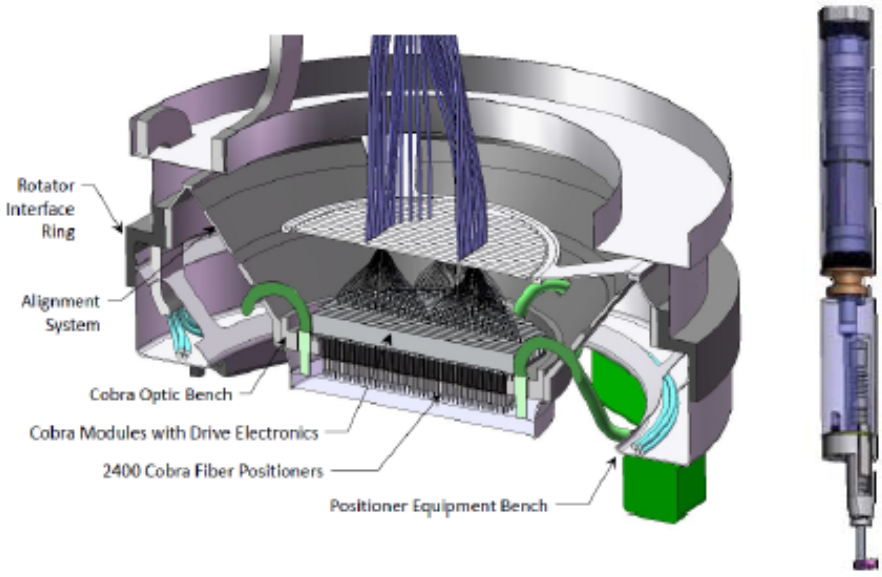

Figure 4.5: The "COBRA" Fiber Positioner designed for WFMOS (left). The tip of the fiber is held at the bottom end of the unit positioner (right). LAMOST uses a design similar to this.

Some infrastructure is required to operate the fiber positioner. Any design requires a system to measure the fiber position during configuration so that the position can be verified to be correct within about 10 microns. The fibers are moved into position and then back-illuminated. Next, a camera is used to check the new position of the fiber. This process is iterated up to 7 times. The total configuration time is expected to be 60 to 90 seconds. We will still need to have Guide and Focus capability, and this may be accomplished by having a small number of CCDs in the DESpec focal plane.

Draft: Do not c ute

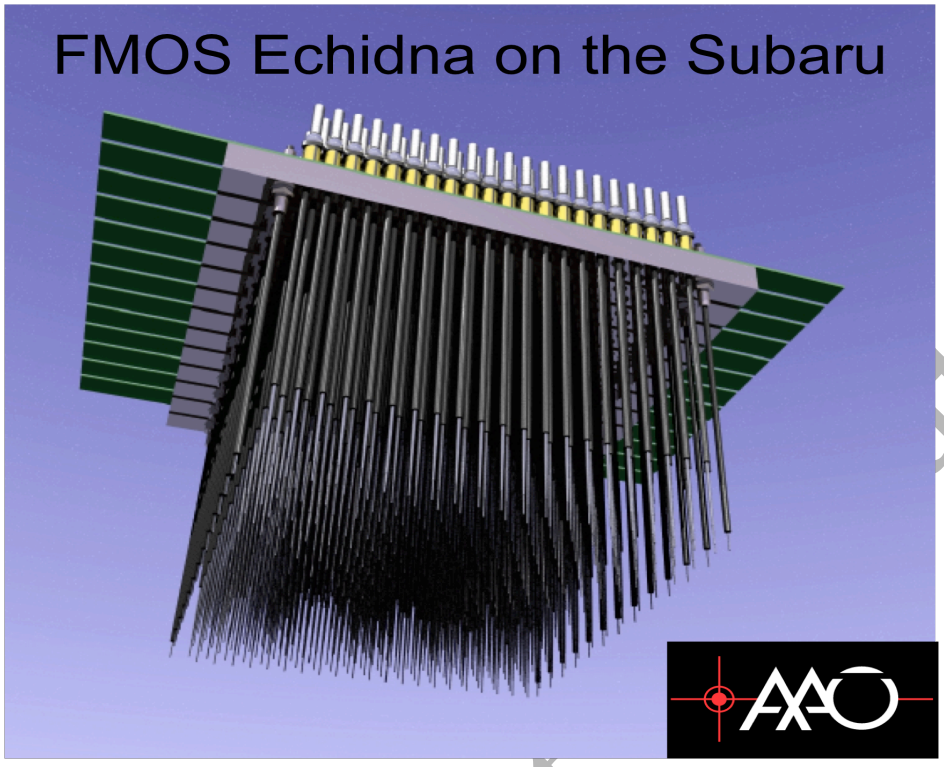

Figure 4.6: The Echidna Fiber Positioner. This instrument is currently operated on the Subaru Telescope. The 400 spines have a 7 mm pitch and can currently be configured for a new target list in ~10 minutes time.

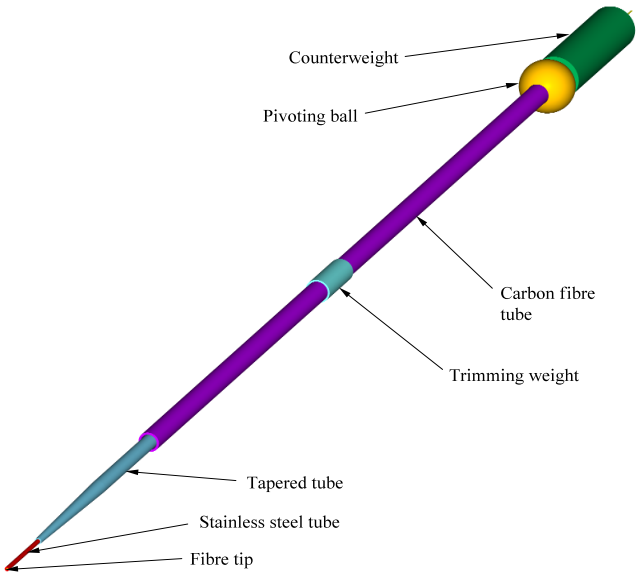

Figure 4.7: The Echidna Unit Fiber Positioner. The spines pivot from mounts at the base and are driven by piezo-electric actuators.

not Dr ate

4.2.3 R&D for the Fiber Positioner

Both the tilting spine and twirling-post approaches produce viable designs for DESpec, with a varying degree of R&D. In either case, R&D would be aimed at decreasing the pitch, increasing the overall light throughput, and decreasing configuration time.

4.3 DESpec Unit Spectrographs and Optical Fibers

DESpec spectrographs will separate the light into component wavelengths and focus it onto CCDs. The key elements driving the optical design of the spectrographs are the wavelength range, the required spectral resolution, and the diameter of the optical fibers carrying the light from the focal surface. To accommodate 4000 fibers, each of 10 spectrographs must accept ~400 fibers. There are several options for the physical location of the spectrographs: they could be mounted off-telescope or, if sufficiently small and light-weight, they could be mounted near the top of the telescope and arrayed around its upper ring in order to minimize fiber length and thereby increase the throughput of the instrument.

As we are still exploring the science and survey requirements at this time, we are considering two spectrograph designs. The first design is a single-arm spectrograph with a wavelength range $550<\lambda<950$ nm or $600<\lambda<1000$ nm. The second is a two-arm spectrograph in which the blue side has wavelength range $500<\lambda<760$ nm and the red side covers $760<\lambda<1050$ nm.

4.3.1 Single-Arm (VIRUS) Spectrographs

The DESpec unit single-arm spectrograph optical design is based on VIRUS, the instrument being built for the HETDEX survey (Hill, et al. 2008) on the 11-meter Hobby-Eberly telescope in Texas. HETDEX requires 200 of these spectrographs, so they must be inexpensive and simple enough to produce in bulk. The VIRUS design (Hill, et al. 2010, Marshall, et al. 2010) is a high-throughput, single-arm spectrograph. Figure 4.8 shows the optical design for VIRUS, which can be easily optimized for the DESpec wavelength regime and spectral resolution.

The VIRUS instruments are composed of a main spectrograph body, which houses the "collimator" and the "disperser" of the spectrograph, and a vacuum vessel that houses a Schmidt-type camera. A volume phase holographic (VPH) grating acts as the dispersing element. The collimator unit consists of a spherical collimator mirror, folding flat mirror, and the VPH grating. The Schmidt camera consists of an aspheric corrector lens that serves as the Dewar window, a spherical camera primary mirror, an aspheric field flattener lens, and a CCD detector that is held in the center of the camera on a spider assembly.

DESpec, like VIRUS, is a set of simple, fixed spectrographs with no moving parts. This feature of the instrument makes it inexpensive, quick to assemble, and easy to mount on or near the telescope.

Draft: Do not circulate

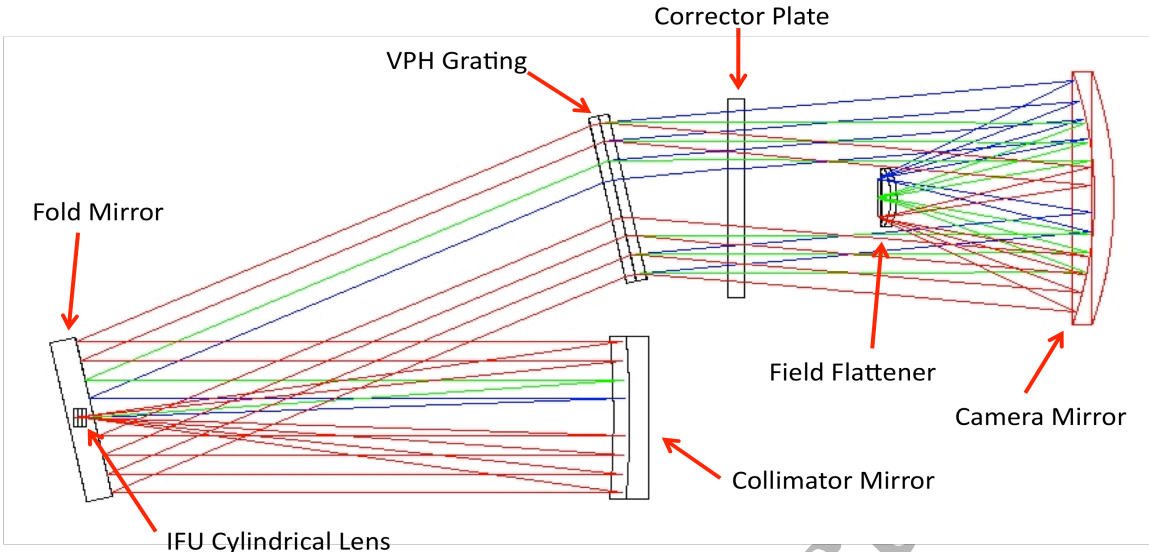

Figure 4.8: Optical layout of one of the VIRUS unit spectrographs. Light enters on the left and is reflected by the collimator mirror and fold mirror before it passes through the VPH grating. The CCD is just to the left of the field-flattener lens. The overall length of the VIRUS is 0.75m.

With the single-arm spectrograph design we use 80 μm diameter (1.4") fibers with a 3 pixel/fiber resolution. That requires an f/1.6 camera. For comparison the HETDEX VIRUS has f/1.33, but still a reasonable optical system. We would use 20 DECam red-sensitive, fully-depleted CCDs, two for each spectrograph. Each spectrograph would have 400 fibers, 200 per CCD, with spectrum along the 4k direction. Table 4.1 lists some of the parameters for the default single-arm spectrograph design (A) and a bluer version (B) in case that is required by the survey.

Parameter	**Single-Arm Spectrograph (A)**	**Single-Arm Spectrograph (B)**
Fiber Diameter	80 μm (1.4")	80 μm
Wavelength Range (nm)	600<λ<1000	550<λ<950
CCD	DECam 2kx4k	DECam 2kx4k
Resolution(Δλ nm/pixel) (use 4000 pixels)	0.1	0.1
# pixels/fiber	3	3
Camera f/#	f/1.6 = = (2.9*45/80)	f/1.6
Spectral Resolution	3334 @ 1000 nm	3167 @ 950 nm
Camera Type	VIRUS	VIRUS

Table 4.1. The one-arm spectrograph default design (A) and a version (B) with a wavelength range shifted 50 nm to the blue.

Draft. Do not circ

4.3.2 Two-Arm Spectrographs

The two-arm spectrograph design would enable an increase in the wavelength range, improve the spectral resolution, and allow an increase in the diameter and thus the total light collected by the optical fibers. These improvements occur because we spread the light out over twice as many pixels (CCDs).

Parameter	**Blue Side**	**Red Side**
Fiber Diameter	100 μm (1.75")	
Wavelength Range (nm)	500<λ<760	760<λ<1050
CCD	E2V or DECam 2kx4k	DECam 2kx4k
Resolution(Δλ nm/pixel) (use 4000 pixels)	0.065	0.0725
# pixels/fiber	5	4
Camera f/#	f/2.2	f/1.7
Spectral Resolution	1923 @ 625 nm	3276 @ 950 nm 3621 @ 1050 nm
Camera Type	Reflective or refractive	

Table 4.2. An example of a two-arm spectrograph with higher resolution on the red side than on the blue side is given. The break at 760 nm is to separate the two spectra at the location of a sky absorption feature.

Parameters for a two-arm spectrograph covering the wavelength range 500 < λ < 1050 nm are shown in Table 4.2. The spectral resolution of the blue side is 1923 at 625 nm. This is sufficient resolution to easily separate the redshifted 3237A OII doublet, which requires R>1200. The spectral resolution of the red side is higher, to allow better subtraction of night sky lines from the science spectrum. An example of a spectrograph of approximately this design was proposed for WFMOS. It is a high-throughput, 2-arm spectrograph with all-refractive optics and VPH gratings (Smee, et al. 2006). Another example of this type of design is the conceptual design proposed for the GMACS wide-field, multi-object optical spectrograph for the Giant Magellan Telescope. GMACS would use a fully refractive spectrograph (Marshall, et al. 2011) divided into a blue and red channel by a dichroic. VPH gratings disperse the light. Five (six) lenses focus the red-side (blue-side) of the light onto CCDs, which are at the end of each optical train. The DESpec version would be scaled down to an appropriate physical size. The benefit of a design such as GMACS is the maximal throughput of the system, in part because the beam is not occulted by a CCD in the center of the camera, and the increased wavelength coverage and/or spectral resolution.

Draft. Do not circulate

4.3.3 Optical Fibers

The light is carried from the fiber positioner to the spectrographs in optical fibers. The diameter of the fibers depends on the expected source flux distribution and the sky background and should be chosen to maximize the S/N ratio of a sky-dominated object spectrum.

The median delivered point-spread-function (PSF) of the Mosaic-II prime focus camera on the Blanco (soon to be replaced by DECam) is 0.9", and the plate scale at the focal plane is 0.27"/15 micron pixel. This suggests that DESpec should use ~1.5 arcsec fibers in order to capture most of the light from faint galaxies while minimizing sky background. We have initial results from a study that optimized the fiber diameter for a flux-limited survey in the presence of a dominant sky background. The calculations start with a magnitude limit and compute the total number of galaxies per sq. degree at this limit. Next a fiber diameter is chosen, and the rate at which spectra are collected to a pre-determined S/N ratio as a function of galaxy magnitude and radius is calculated. The distribution of galaxy radii and magnitudes comes from the COSMOS simulation (Jouvel, et al. 2009), as described in Sec. 3. Because large galaxies tend to have low surface brightness, they are the most difficult spectroscopic targets. The rates are calculated using a weighted average over a distribution of CTIO-measured seeing. A contribution of 0.6" from the optics PSF is included. For magnitude limits in the range 22 to 24, the optimal fiber size is in the range 1.8 to 2.0 arcsec. However, the rate at which redshifts are collected depends only weakly on fiber size: the range in fiber sizes that have success rates within 10% of the peak rate correspond to diameters ranging from 1.5 to 2.4 arcsec. The intersection of these ranges that is near-optimal for all limiting magnitudes is 1.7 to 2.1 arcsec. Because the optimization has determined that the fiber diameter is a soft minimum, we expect that the final diameter can be selected based largely on other considerations, such as spectrograph resolution or fiber positioning accuracy.

The input f-ratio, f/3, is ideal for high-efficiency in capturing the light and for high throughput and low focal ratio degradation (Murphy, et al. 2008). The length of the fibers is 10 to 30 meters and depends on where we mount the spectrographs. Figure 4.9 shows fiber throughput versus fiber length for six different wavelengths from 500 to 1100 nm in a typical fiber. Finally, we note that several fibers per spectrograph will point at blank sky to measure the sky spectrum for sky subtraction.

4.3.4 R&D

R&D in this area will lead to a design for the DESpec unit spectrograph and its optics. The choice among designs will come from the science and survey requirements. The R&D will optimize the fiber diameter (for instance, sky-background in some wavelengths suggests smaller fibers improve the signal-to-noise), fiber length, light throughput, and signal-to-noise ratio of the observations. We would also determine how many fibers could be read out on each CCD. An

Draft: Do not circulate

increase here could decrease the number of spectrographs by 30%, and therefore, the total cost. In addition, there is substantial R&D being performed around the world on concepts (e.g. Content & Shanks 2008; Content et al. 2010) for multiobject spectroscopic instruments on wide-field telescopes. We are watching these efforts carefully in case a sensible technical alternative for the DESpec arises.

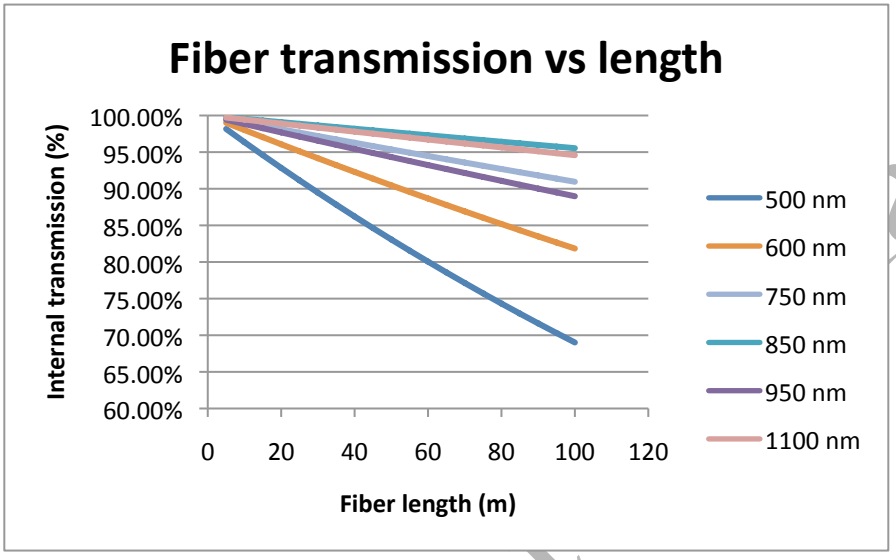

Figure 4.9: Fiber throughput versus fiber length at six different wavelengths for Polymicro broadband fibers. This assumes optimal f-number, which is f/3 to f/4. Note that for shorter wavelengths the fibers have a lower throughput, which gets progressively worse for λ<500 nm.

3.4 CCDs and Readout

3.4.1 CCDs

The light will be dispersed by the spectrographs onto CCDs. DESpec will use 2k x 4k backside-illuminated, red-sensitive CCDs designed by LBNL, for either the one-arm spectrograph or for the red side of the two-arm spectrograph. These CCDs have high quantum efficiency (QE) at near infrared wavelengths. They are 250 microns thick and attain good (~5 micron) dispersion characteristics from a 40V substrate bias. The 4-side buttable CCD package is suitable, so existing spare, tested, packaged, science-grade DECam CCDs (Estrada, et al. 2010) can be used on DESpec, providing a significant cost saving, although we include their costs for the purpose of making cost estimates at this time. Figure 4.10 shows the quantum efficiency of 3 CCDs produced for DECam.

Draft. Do not circulate

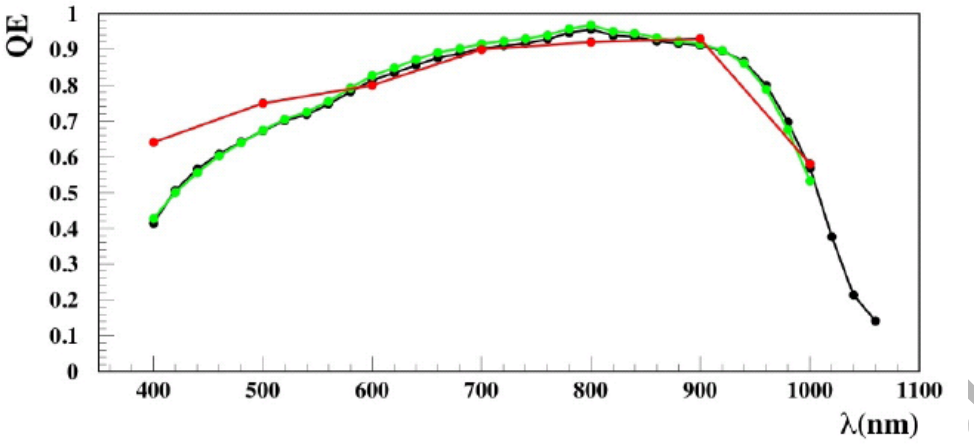

Figure 4.10: The absolute QE of three typical CCDs produced for the Dark Energy Camera.

The blue side of the two-arm spectrographs could also use DECam 2kx4k CCDs. E2V 2kx4k devices would also work and have QE that is a little better around 500 nm.

The DECam CCD readout electronics, which can read out the 2kx4k CCD in ~17 (45) seconds with ~10 (3) electrons/pixel noise, satisfies all of DESpec's requirements. It could be modified relatively easily for the E2V CCD if necessary. Ongoing R&D at Fermilab on low-read-noise techniques might reduce the readout noise to well under 1 electron/pixel, should that be desirable.

4.5 Interchangeability with DECam

The Dark Energy Camera has been designed for efficient installation and removal from the Prime Focus Cage. Figure 4.11 shows the camera installation fixture positioned in front of the Prime Focus Cage, mounted on the Telescope Simulator at Fermilab (Diehl, et al. 2010). To change from DECam to DESpec, one tilts the Blanco over to the northwest platform and uses the camera installation fixture to remove DECam. DECam is then stowed off of the telescope with its Dewar window, the camera's final optical element (C5), in place. DESpec, which will have been stowed either off-telescope or on the telescope structure, is connected to a similar installation fixture for inserting into the cage. DESpec would be approximately the same weight as DECam; differences in weight would be corrected-for by adjustment of the prime focus cage counterweights.

The DECam Project is supplying CTIO with a platform that allows easy installation and removal of the filter-changer and shutter. The platform is with the telescope at the North position. DESpec's ADC and (the same) shutter will be installed and removed from the same platform using a similar procedure.

Draft: Do not circulate

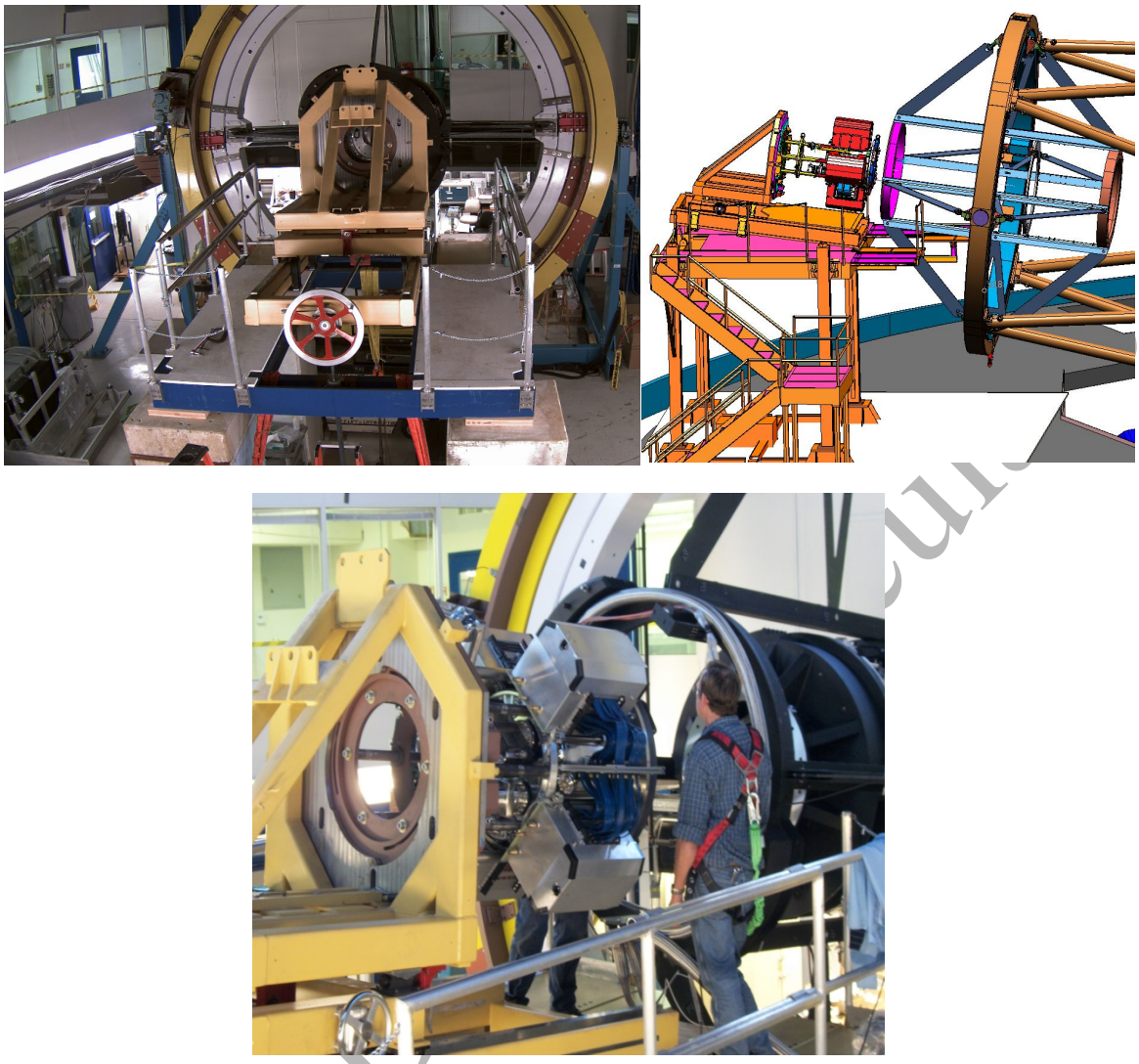

Figure 4.11: The camera installation fixture (in the foreground at top left, schematic at top right, in close-up at bottom) at Fermilab. Bottom image shows the installation fixture being used to mount the camera in the Prime Focus Cage (black, at right). The cage itself is attached by fins to the white and yellow rings of the telescope simulator; the inner white ring has the same dimension as the ring at the top end of the Blanco. The simulator was used to test DECam in all configurations it will encounter on the telescope as well as the mounting and dismounting procedures.

4.6 The Blanco Telescope

The Blanco 4m telescope was named after Dr. Victor M. Blanco (1918-2011), an astronomer from Puerto Rico, who was the second Director of CTIO (1967-1981). The Blanco is an equatorial mount telescope with a 150” diameter primary mirror. The primary mirror and prime focus cage are mounted on a Serrurier Truss (Abdel-Gawad, et al. 1969). The telescope was commissioned in 1974 (Blanco 1993). Until 1998, it was the largest telescope in the Southern

Hemisphere. It has a high-quality Cervit primary mirror that provides excellent image quality. An extensive set of improvements made a decade ago included replacement of the passive primary mirror supports with an active system and alterations to the telescope environment to improve the air flow and remove heat sources. More recent improvements made for the Dark Energy Camera include replacement of the primary mirror's radial supports, which has substantially reduced motion of the primary in its cell, and an upgrade of the telescope control system. Figure 4.12 shows a photograph of the Blanco 4m telescope with its original prime focus cage (to be replaced by the DECam prime focus cage in late 2011).

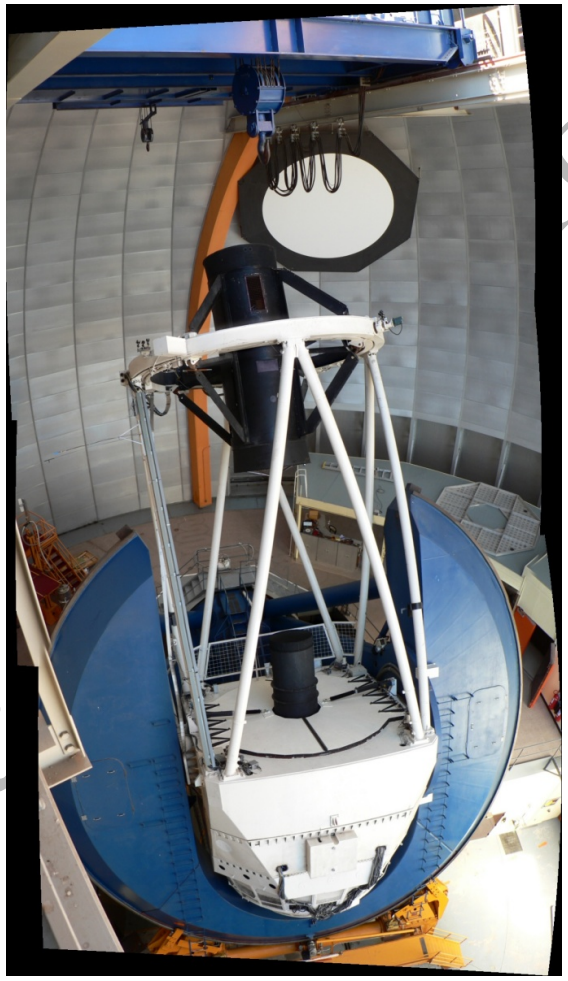

Figure 4.12: The Blanco 4m telescope.

Draft. Do not circulate

4.7 Technical Summary

We have described technical solutions to the DESpec design and demonstrated that there are no technical "show-stoppers". For the major new systems, we have provided examples that have already been designed and built for existing or near-term instruments. While these are not final technical choices, they do represent solutions that satisfy our project scope and goals with minimal R&D.

We have estimated that this instrument is approximately the same scale project as DECam and can be built at roughly the same cost and on similar timescale. Members of this team have completed the $35M DECam Project on budget and on schedule. Installation of that instrument is now ongoing at Cerro Tololo, in Chile. Our experience with DECam has guided our estimate for the DESpec cost and schedule. Our approximate DESpec cost estimate includes costs for the new components (~$19M), and costs for management, survey planning, and unspecified mechanical integration, totaling $6M. On top of that we include 50% contingency, because the design and scope are still under development and will be optimized based on the scientific case. Including the contingency, the total DESpec construction cost is expected to be ~$39M. Some factors may mitigate portions of the cost. There will be a significant number of red-sensitive CCDs left over from DECam construction and these may be useful for some or all of DESpec's requirements. It is possible, even likely, that substantial costs will be defrayed through the contribution of university- and international collaborators, as was the case with DECam.

5. Conclusion

This White Paper has presented the science motivation, an initial concept, and technical options for the Dark Energy Spectrometer. DESpec would be a unique instrument that would make a major advance in our understanding of dark energy and the origin of cosmic acceleration and would enable powerful tests of General Relativity on cosmic scales. It would significantly enhance the scientific reach of DES in the near term and LSST in the longer term and would in addition make possible an array of new scientific studies by the astronomy community. Moreover, it would build upon and make use of the infrastructure built for the Dark Energy Camera, achieving substantial cost savings and reducing technical and schedule risks.

Appendix: DESpec and BigBOSS

As noted above, the combination of DESpec in the south and BigBOSS in the north would enable spectroscopic surveys over essentially the entire sky, maximizing the DE constraints that could be pursued from the ground. Here, for context we briefly compare and contrast the DESpec and BigBOSS designs. BigBOSS is a proposed 5000-fiber spectrograph system for the Mayall 4-meter telescope at Kitt Peak National Observatory in Arizona (Schlegel, et al. 2011). The Mayall and Blanco telescopes are essentially identical mechanically, and both observatories are operated by NOAO. The BigBOSS design calls for a larger field of view (FOV) than DESpec

Draft. Do not circulate

(7 vs. 3.8 sq. deg.), requiring several larger optical corrector elements and entailing an entirely new prime focus cage, active alignment system, and set of corrector lenses for the Mayall. The BigBOSS robotic fiber system would be similar to that used for the LAMOST project in China; it has a larger pitch (inter-fiber physical separation) that is technically less challenging to achieve. BigBOSS would employ multi-arm spectrographs to span a broader range of wavelengths (extending down to 340 nm, to access the Lyman-alpha forest along QSO sight-lines) at slightly higher spectral resolution than currently envisioned for DESpec. BigBOSS is optimized to probe Baryon Acoustic Oscillations (BAO) to redshifts $z>1$ and would select spectroscopic targets mainly from WISE (infrared), Palomar Transient Factory (PTF), and PanSTARRS imaging, which are shallower than DES. Given its location at relatively high latitude, BigBOSS would be able to target only ~500 sq. deg. (~1/10) of the nominal DES survey area and up to ~several thousand sq. deg. of the LSST footprint, so it would not take full advantage of the synergy between weak lensing (DES, LSST) and redshift-space distortions from the same volume (Sec. 2) nor would it be able to follow up the majority of DES and LSST targets. The deep, multi-band, precisely calibrated photometry from DES and LSST should in principle enable more efficient spectroscopic targeting, a topic requiring further study. On the other hand, the DES and BigBOSS collaborations are currently jointly exploring the possibility of increasing the area overlap between DES/DECam imaging and BigBOSS spectroscopy through increased survey time in the celestial equator regions; an overlap of up to several thousand sq. deg. may be possible but would require DECam imaging time beyond that allotted to the DES project.

In order to reach the density of galaxy targets optimal for BAO studies, BigBOSS would revisit each field several times. DESpec, with a higher density of fibers on the sky, would reach the same target density in fewer visits. However, since DESpec has a smaller FOV, the two instruments would in fact have comparable speed (number of targets per unit area per unit time) for a BAO-optimized survey. BigBOSS proposes to measure ~20 million galaxy redshifts over 14,000 sq. deg. in 500 nights. Conservatively assuming longer cumulative exposure times to ensure redshift success, we estimate that DESpec could measure ~7 million redshifts over 5000 sq deg. in ~300 nights and by extension ~20 million redshifts over 15,000 sq. deg. with DES+LSST imaging in ~900 nights. DESpec would enable many other follow-up programs over the entire 20,000 sq. deg. LSST survey area as well. Given the site conditions, DESpec would be expected to have a higher fraction of useable nights than BigBOSS (~80% vs. ~65%) and better seeing (median delivered to the Blanco 0.9” compared to 1.1” for the Mayall).

The BigBOSS proposal of Oct. 2010 responded to an NOAO Announcement of Opportunity for a new instrument for the Mayall telescope; in Jan. 2011, the Large Science Program panel that reviewed the proposal recommended that NOAO work with the BigBOSS team to further develop the proposal, retire key risks to the project, and bring it to a state of readiness for submission to DOE. As indicated in Sec. 1, NOAO has no plans to issue an announcement of opportunity for a new instrument for the Blanco.

Draft. Do not circulate

References

Abdalla, F., et al. 2008, MNRAS, 387, 945
Abdel-Gawad, M. K. 1969, KPNO-CTIO Engineering Dept. Technical Report #9
Akiyama, M., et al. 2008, Proc. SPIE Vol 7018, 70182V
Albrecht, A., et al. 2006, Report of the Dark Energy Task Force, astro-ph/0609591
Albrecht, A., et al. 2009, Findings of the Joint Dark Energy Mission Figure of Merit Science Working Group, arXiv: 0901.0721
Albrecht, A., & Bernstein, G. 2007, Phys. Rev. D75, 103003
Bernstein, G. & Cai, Y. 2011, arXiv:1104.3862
Bernstein, G. & Huterer, D. 2010, MNRAS, 401, 1399
Blake, C. & Glazebrook, K. 2003, ApJ, 594, 665
Blanco, V. 1993, http://www.ctio.noao.edu/diroff/ctio_history.htm
Blanton, M.R., & Roweis, S. 2007, AJ, 133, 734
Capak, P. et al. 2007, ApJS, 172, 99
Capak, P. et al. 2009, in preparation
Coe, D. et al. 2006, AJ, 132, 926
Collister, A. & Lahav, O. 2004, PASP, 116, 345
Content, R., & Shanks, T. 2008, Proc. SPIE Vol 7014, 701475
Content, R. et al. 2010, Proc. SPIE Vol 7735, 77351Q
Cunha, C. 2009, Phys. Rev. D79, 063009
D'Andrea, C., et al. 2011, submitted
DES Collaboration 2005, astro-ph/0510346
Diehl, H. T., et al. 2010, Proc. SPIE Vol 7735, 7735125
Dvali, G., Gabadadze, G., & Poratti, M. 2000, Phys. Lett. B, 485, 208
Eisenstein, D., et al. 2001, AJ, 122, 2267
Eisenstein, D., et al. 2005, ApJ, 633, 560
Estrada, J., et al. 2010, Proc. SPIE 7735, 77351R
Frieman, J., Turner, M. S., & Huterer, D. 2008, Ann. Rev. Astron. Astrophys., 46, 385
Gaztanaga, E., Eriksen, M., et al. 2011, in preparation
Giavalisco, M. et al. 2004, ApJ, 600, 103
Gupta, R., et al. 2011, submitted
Guzik, J., Jain, B., & Takada, M. 2009, arXiv:0906.2221
Hanuschik, R.W. 2003, A&A, 407, 1157
Hill, G. J., et al. 2008, ASPC, 399, 115
Hill, G. J., et al. 2010, Proc. SPIE Vol 7735, 77350L
Huterer, D., Takada, M., Bernstein, G., & Jain, B. 2005, MNRAS, 366, 101
Ilbert, O. et al. 2009, ApJ, 690, 1236
Jouvel, S., et al. 2009, A&A, 504, 359

Draft. Do not circulate

Kaiser, N. 1987, MNRAS, MNRAS, 227, 1
Kelly, P., Hicken, M., Burke, D., Mandel, K., & Kirshner, R. 2010, ApJ, 715, 743
Kennicutt, R.C. 1998, ApJ 498, 541
Kirk, D., Lahav, O., Bridle, S., et al. 2011, in preparation.
Kurtz, M.J., & Mink, D.J. 1998, PASP, 110, 934
Lahav, O., Kiakotou, Abdalla, F., & Blake, C. 2010, MNRAS, 405, 168
Lampeitl, H., et al. 2010, ApJ, 722, 566
Le Fèvre, O. et al. 2005, A&A, 439, 845
Ma, Z., Hu, W., & Huterer, D. 2006, ApJ, 636, 21
Marshall, J. L., et al. 2010, Proc. SPIE 7735, 77354J
Marshall, J. L., et al. 2011, AAS Meeting #217, #433.12
Matthews, D. & Newman, J. 2010, ApJ, 721, 456
McCall, M. et al. 1985, ApJS, 57, 1
McDonald, P., & Seljak, U. 2009, JCAP, 10, 7
Moustakas, J. and Kennicutt, R.C. 2006, ApJS, 164, 81
Mouhcine, M. et al. 2005, MNRAS, 362, 1143
Muller, G. P. 2008, Proc. SPIE Vol 7014, 70144R
Murphy, J. D., et al. 2008, Proc. SPIE Vol 7018, 70182T
Newman, J. 2008, ApJ, 684, 88
Pen, U. 2004, MNRAS, 350, 1445
Perlmutter, S., et al. 1999, ApJ, 517, 565
Ramsey, L. 1988, in Proc. of the Conf. on Fiber Optics in Astronomy, Tucson, AZ
Reyes, R., et al. 2010, Nature, 464, 256
Riess, A., et al. 1998, AJ, 116, 1009
Schlegel, D., et al. 2011, arXiv:1106.1706
Seiffert, M. 2009, presentation at Princeton University
Seo, H., & Eisenstein, D. 2003, ApJ, 598, 720
Smee, S., et al. 2006, Proc. SPIE, Vol 6269, 6269I-3
Song, Y., & Dore, O. 2009, JCAP, 0903, 025
Song, Y., et al. 2011, arXiv: 1011.2106
Sullivan, M., et al. 2010, MNRAS, 406, 782
Sullivan, M., et al. 2011, arXiv: 1104.1444
Thomas, S., Abdalla, F., & Lahav, O. 2010, Phys. Rev. Lett. 105, 031301
Thomas, S., Abdalla, F., & Lahav, O. 2011, Phys. Rev. Lett. 106, 241301
Wu, H., Rozo, E., & Wechsler, R. 2010, ApJ, 713, 1207
Zhang, P., Liguori, M., Bean, R., & Dodelson, S. 2007, PRL, 99, 141302
Zhao, G., et al. 2010, Phys. Rev. D, 81, 103510

Draft: Do not circulate